Bachelor Thesis

Synthesis and Characterization of Novel Supramolecular Polymers

By Pascal Mulder

6/28/2018

Accomplished at the University of Groningen

Faculty of Science and Engineering

Zernike Institute for Advanced Materials

Macromolecular Chemistry and New Polymeric Materials

ACKNOWLEDGEMENT

Under the supervision of prof. dr. K.U. Loos and M. Golkaram

To express my gratitude, I would like to thank a few people who helped me during my thesis. First of all, I would like to thank prof. dr. K.U. Loos for the opportunity to do my bachelor research project at the Macromolecular Chemistry and New Polymeric Materials division. Secondly, I would like to thank M. Golkaram, for his great help and supervision during my project. Also, I would like to thank A.J.J. Woortman for the GPC measurements and J. van Dijken for the DSC and TGA measurements.

Table of Contents

Abstract

The goal of this thesis was to synthesize and characterize supramolecular polymers with unique structures; namely, star or brush shaped architectures. First a supramolecular star core was tried to synthesize. The hydrogen bonding thymine stickers were attached to the core with a copper-catalyzed azide-alkyne cycloaddition (CuAAC) click reaction. From ^{1}H NMR analysis a conversion of 53 % could be determined. This means that each star core has only one or two thymine end-groups instead of three. Since, the product could not be isolated with column chromatography, it could not be used to form a supramolecular star network.

Next, a brush shaped supramolecular polymer was synthesized starting from the synthesis of a 2,7-diamide-1,8- naphthyridine (Napy) based sticker. During the synthesis all steps except the final step resulted in a quantitative yield. In the final step, the double bond of the monomer was introduced by reacting 1-(6-isocyanatohexyl)-3-(7-oxo-7,8-dihydro-1,8-naphthyridin-2-yl)urea with 2-hydroxyl acrylate. This reaction was catalysed by dibutyltin dilaurate (DBDTL) and the product was obtained in a 66 % yield. The Napy monomer was polymerized using a reversible addition-fragmentation chain-transfer (RAFT) polymerization. Using 2-(Dodecylthiocarbonothioylthio)-2-methylpropionic acid (DDMAT) as chain transfer agent (CTA), a polymer with $\overline{M_n}$ = 4,050 was obtained. The thermal properties were determined with thermographic analysis (TGA) and differential scanning calorimetry (DSC). From the measurements it could be concluded that a high glass transition temperature (T_g) polymer was obtained with a decomposition temperature of 238.4 °C.

Also, a copolymer with different compositions was synthesized from the Napy-based monomer and n-butyl acrylate by a RAFT polymerization using *S*,*S*-Dibenzyl trithiocarbonate (DBTTC) as CTA. The thermal properties were compared with pure poly (n-butyl acrylate). DSC confirmed that the T_g of the copolymers increased with increasing amounts of Napy side groups, which is a result of the increasing hydrogen bonding interactions.

Eventually, the Napy-based polymers can be used as backbone to create a well-defined supramolecular brush network with ureidopyrimidinone (UPy) based side chains, introducing new properties to the field of supramolecular polymer chemistry.

Introduction

Background

The synthesis of polymeric networks has been appealing because they have many interesting properties such as different self-assembly behaviour and chain relaxation. However, conventional polymeric structures lack dynamic properties such as reversible cross-linking. This property can be introduced by adding non-covalent interactions, like hydrogen bonding, to the polymer or monomer. With these non-covalent interactions, a supramolecular network can be created.

After Lehn *et. al.* started the field of supramolecular chemistry in 1978, the interest in the field of supramolecular chemistry has grown and therefore it is now an established discipline of chemistry.[1] This discipline scales from membranes to gels, vesicles, monolayers and fibres.[2] In polymer chemistry, the focus is mainly on the formation of supramolecular architectures by non-covalent interactions, such as H-bonding, π-π stacking and ligand-metal complexation, which all have been studied in recent years.[3]

The supramolecular polymers show three interesting properties. First of all, the (macro)monomers assemble themselves into the polymeric(network), without using a catalyst or an initiation process. Secondly, during the polymerization, dynamic termination processes are occurring. And finally, the polymerization or crosslinking processes are dynamic, which means that they are reversible.[4] The dynamic nature of the supramolecular polymers makes the materials useful for liquid crystalline materials, light harvesting systems, biomolecular materials and block copolymer assemblies.[1], [5], [6]

A consequence of the dynamic behaviour of the supramolecular polymers is that the strength of the supramolecular interactions between the monomers highly influences the degree of polymerization. Therefore, supramolecular polymers are very responsive to changes in temperatures and their melt viscosities show sharp dependence on temperature. This creates the possibility to shift the equilibrium to the monomer side on demand by exposing an appropriate stimulus to the material. By doing this, the molecular weight of the supramolecular assemblies can be temporarily reduced and if the system is under sufficient dynamic control, healable polymers can be created.[3]

Also, cases exist in which a polymer backbone contains hydrogen bonding side chains, giving a brush like structure. Here, hydrogen bonding interactions can be used to accommodate better interfacial properties and may eventually lead to blending of a normally immiscible polymer pair.[7] In this way, the properties of the polymer blend can be tuned by varying the mole percent of the hydrogen bonding moieties. Also, different hydrogen bonding moieties can be introduced to increase or decrease the strength of the interactions between the polymer chains.[7]

The problem with current research on supramolecular polymers is that most supramolecular polymers have been made in solution, while for a mechanical robust product the polymer is needed in the molten state. In order to have a well-defined morphology, the system has to

be well-defined too. This can be created by, for example, supramolecular networks formed from brush or star shaped architectures with hydrogen bonding moieties attached to linear polymer chains.

Incentives and objectives

The aim of this research is to synthesize and characterize supramolecular polymers with unique structures; namely, star and brush shaped architectures. The synthesis of these new supramolecular architectures can be used to create supramolecular networks, which can introduce new properties to the field of supramolecular chemistry.

First a supramolecular star core is synthesized starting from trimethylol propane triglycidyl ether **1**.[8] The supramolecular interactions are created by the attachment of hydrogen bonding moieties based on the thymine functional group **3** directly to the star core by a copper catalysed click reaction. The thymine functional groups are able to form hydrogen bonds with complementary hydrogen bonding moieties, such as diamino triazine (figure 1). A supramolecular network can be formed between the star core with thymine units and linear polymer chains with diamino triazine units. Eventually the thermal and rheological properties of the supramolecular star polymer can be compared with the properties of the conventional star polymers, which have been studied in detail.[9]

The synthesis of the second supramolecular architecture which is aimed in this study is a polymer with Napy-based hydrogen bonding side groups **10**. This monomer is synthesized starting from 2,6-amino pyridine **6** and DL-malic acid **7**. Next hexamethylene diisocyanate (HDI) **9** is introduced as alkyl spacer to the hydrogen bonding end group. And finally, 2-hydroxyethyl acrylate **11** will be added to introduce a vinylic end group for the polymerization.

Raft polymerization will be used to synthesize the homopolymers and copolymers with n-butyl acrylate in different compositions. The composition and molecular weight of the synthesized polymers will be determined by ^{1}H NMR, where the ratio between the chain transfer end group and the monomer units will be used to calculate the molecular weight. Gel permeation chromatography (GPC) will be used to confirm the molecular weight of the polymer and to determine the polydispersity index (PDI). The thermal properties will be determined by DSC and rheology measurements.

Eventually the supramolecular interactions of the synthesized polymer can be investigated in future research by using dynamic light-scattering (DLS) and viscosity measurements. In previous research, the supramolecular interactions between an urea of guanosine and 2,7-diamido-1,8-naphthyridine along a main backbone of poly(butyl)methacrylate and polystyrene are already confirmed and displayed.[7] This study shows that by varying the concentration of quadruple hydrogen-bonding moieties, a polymer blend can be created between two immiscible polymers. The benefit of the strong quadruple hydrogen-bonding complex is that only a low mole percent of comonomers is required. This results in only a small change in the properties of the polymers.

The click reaction and the RAFT polymerization will be explained more in the theory section. Also, information about the role of hydrogen bonding in supramolecular structures can be found in this section. The reactions, observations, results and improvements can be found in the results and discussion. The summary, experimental, and additional spectra can be found at the end of the report.

Theory

Click reaction

For the synthesis of the supramolecular star core, the so called “click reaction” is used to add the hydrogen bonding moieties to the core. In this research a CuAAC click reaction is used, because it suits a broad temperature range, tolerates a large functional group range and is insensitive to a pH range of 4 to 12 and to aqueous conditions.[10]
For the copper catalyst, copper(II)sulfate pentahydrate is used. Sodium ascorbate is added to reduce Cu(II) to Cu(I), which is visible from the change in colour of the reaction mixture. Cu(II) results in a green colour of the mixture, where the reduction to Cu(I) causes the mixture to become yellowish.
The first step in the mechanism, which is depicted in scheme 1, is the coordination of Cu(I) to the alkyne (**1**). After this, the proton of the alkyne is substituted for another Cu(I) (**2**). After the azide comes in (**3**), the σ-copper acetylide and the π-bound copper together coordinate the azide (**4**). This results in a six-membered copper metallacycle, where one copper atom stabilizes the ring. After a triazolyl-copper derivative is formed by ring contraction (**5**), the final product is formed by protonolysis (**6**), which is the final step of the catalytic cycle.[11]

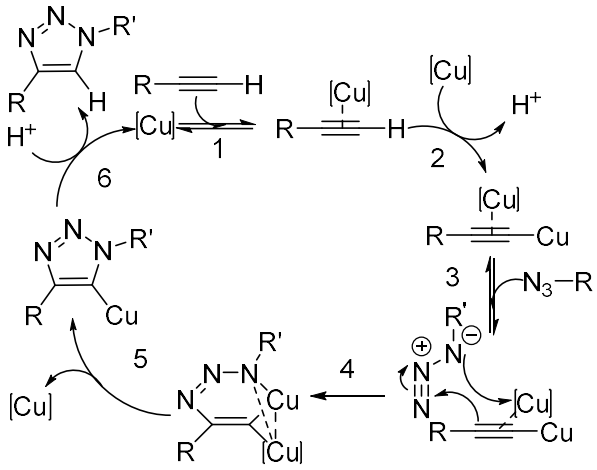

Scheme 1. Mechanism of the CuAAC click reaction [11]

RAFT polymerization

The main polymerization technique used in this study is the RAFT polymerization, which is chosen because it is a versatile process which only needs mild reaction conditions. Furthermore, RAFT is known to give high conversions and a narrow weight distribution.[12]
For a RAFT polymerization, an initiator and a CTA are needed. During this research AIBN is used as initiator and DBTTC and DDMAT are used as CTA (figure 1).

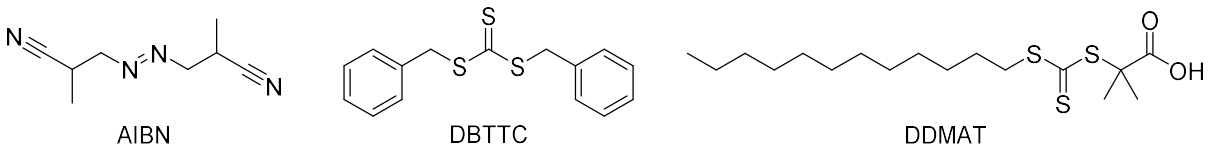

Figure 1. Structures of the initiator (AIBN) and the two CTA's (DBTTC and DDMAT)

When the initiator is exposed to a chemical reaction, electromagnetic radiation or heat, it is cleaved homolyticly into two framents I·. Next the radical fragments react with one monomer unit to start a growing polymeric radical P_1· with length 1 (scheme 2).

Scheme 2. Decomposition of the initiator leading to initiation of the monomer

After initiation, propagation occurs, which is also called chain growth. Here polymer radicals P_n· with length n add to monomer M, forming a longer polymer radical P_{n+1}· (scheme 3).

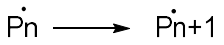

Scheme 3. Propagation of the radical chains

In the RAFT pre-equilibrium, polymer radicals P_n· react with the CTA leading to the formation of a RAFT adduct radical. This is a reversible process, which can lead to a fragmentation reaction in both directions to yield either a radical R· or the starting species P_n· and the polymeric RAFT agent (scheme 4).

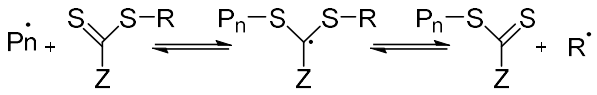

Scheme 4. RAFT pre-equilibrium

The radical R· will react with monomer M and will start a new growing polymer radical P_1· in a process called re-initiation (scheme 5).

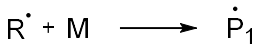

Scheme 5. Re-initiation of the monomer

The most important part of the RAFT polymerization is the RAFT main equilibrium. Here, the present radicals are shared among all species that have not undergone termination yet. The newly formed chains have a narrow poly dispersity index (PDI) and have an equal opportunity for growth, because the present radicals are shared equally between the species that are not terminated yet (scheme 6).

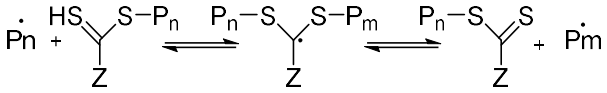

Scheme 6. Raft main equilibrium

Finally, termination occurs for 10 % of the polymer radicals $P_n\cdot$ and $P_m\cdot$ with length n and m respectively, since the concentration of the initiator is 10 % of the concentration of the CTA (scheme 7).[12]

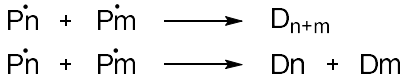

Scheme 7. Termination of the radical chains

Hydrogen bonding

The most important supramolecular interaction in this research is hydrogen bonding. Although hydrogen bonding is usually not very strong (in the order of 10 – 25 kJ mol^{-1}), a cooperation of multiple hydrogen bonds can result in stronger intra- and intermolecular interactions.[13], [14]

In this research, hydrogen bonding moieties, also called stickers, will be added to monomer units. When a polymer is formed from these monomers, the sticker can form a supramolecular network by interacting with other stickers.[15] An example of these interactions in nature is DNA. Here the interactions between cytosine and guanine and between adenine and thymine form the well-known double helix.[16], [17]

Also, in macromolecular chemistry nature is often used as inspiration. An example of this is the thymine-based sticker used for the supramolecular star core, which can interact with diamino triazine (figure 2).

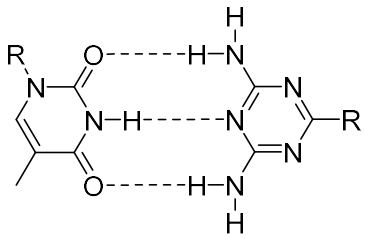

Figure 2. Hydrogen bonding between a thymine-based sticker (left) and a diamino triazine-based sticker (right)

The hydrogen bonding interactions between the thymine-based stickers attached to the supramolecular star core and diamino triazine functionalized linear polymer chains results in a novel supramolecular star shaped architecture (figure 3).

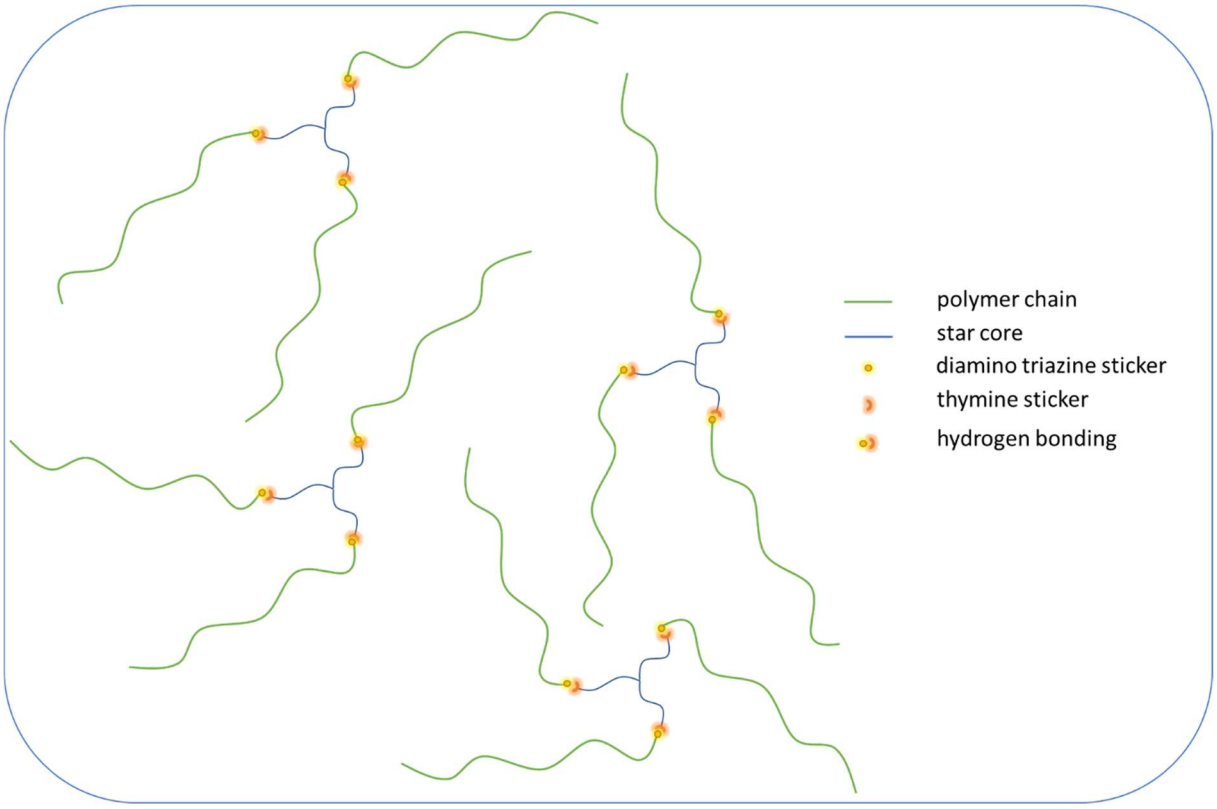

Figure 3. Supramolecular network between the star core with thymine-based stickers and polymer chains with diamino triazine-based stickers

For the synthesis of the hydrogen bonding monomer, a Napy-based sticker was used. This sticker was provided by M. Golkaram and will also be synthesized during this research. The benefit of this sticker is that it is self-complementary, since it is having three donor and three acceptor sides (DADA). This results in six hydrogen bonds, from which four can be formed from bifurcated hydrogen bonds. The proposed hydrogen bonding interactions are depicted in figure 4.

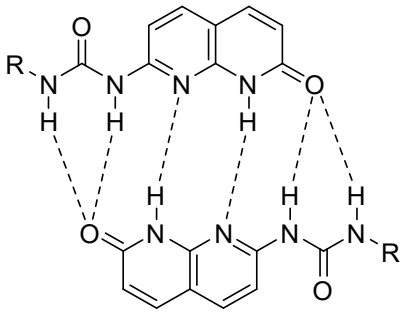

Figure 4. Hydrogen bonding between two Napy-based stickers

It is expected that the Napy-based sticker can also form a strong hydrogen bonding complex with ureidopyrimidinone (UPy) based stickers (figure 5), which were introduced by Meijer *et al*., (2012).[18] This results in two proposed complexes where 4 hydrogen bonds are formed (DAAD and DDAA). These complexes are expected to be stronger than the self-

complementary structures of both stickers, since secondary interactions are formed between the two -NH hydrogen bond donors of UPy and the two -N hydrogen bond acceptors of Napy.

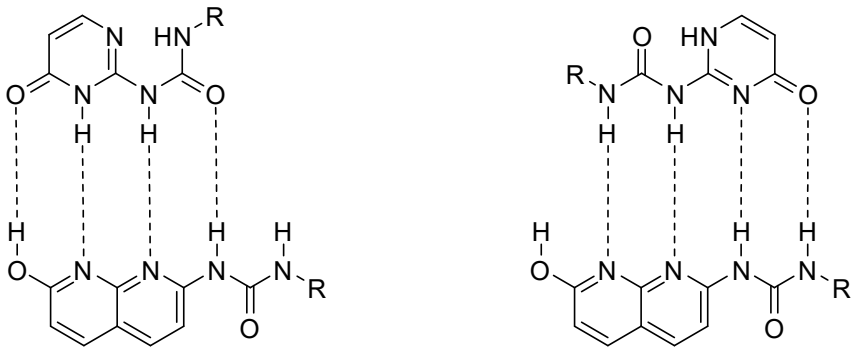

Figure 5. Two proposed conformers resulting from the hydrogen bonding interactions between Napy-based stickers (top) and UPy-based stickers (bottom)

The hydrogen bonding interactions between Napy and UPy can be used two form a novel brush-like supramolecular architecture, which is formed between a polymer backbone with Napy side-groups and UPy functionalized linear polymer chains (figure 6). The linear polymer side chains tend to entangle, resulting in the network formation.

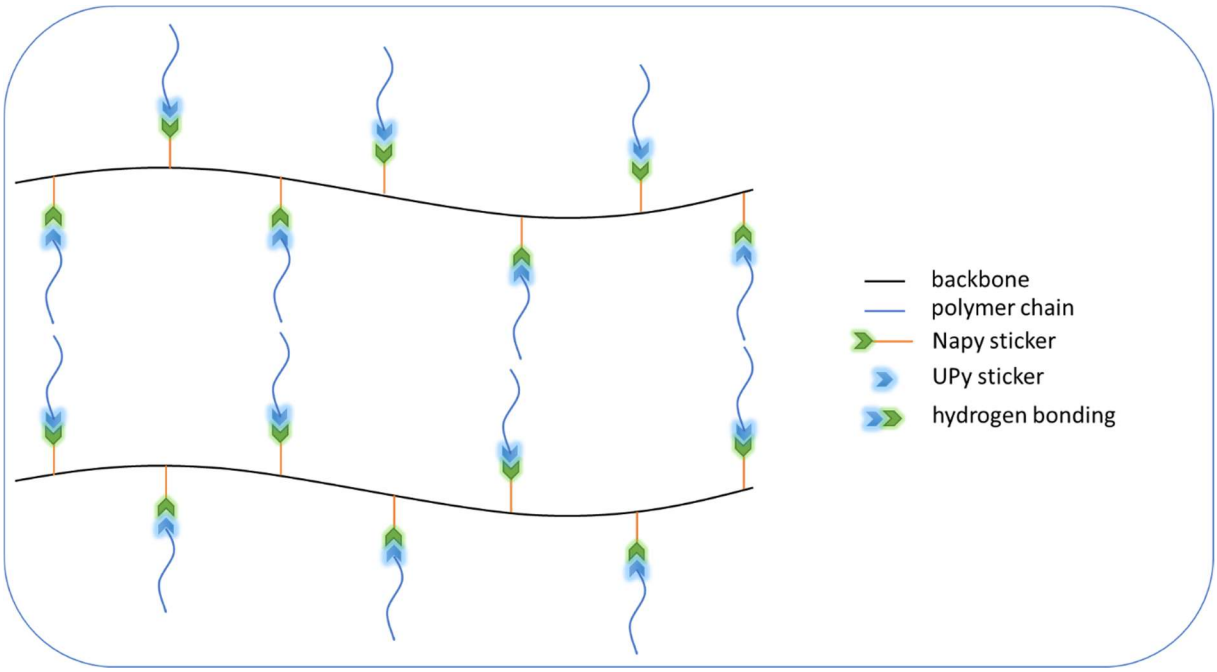

Figure 6. Supramolecular network between a backbone containing Napy-based stickers and UPy functionalized linear polymer chains

In previous research the UPy-based stickers are introduced in poly (n-butyl acrylate), forming a copolymer with different compositions. Increasing the number of hydrogen bonding groups resulted in a linear increase of the T_g.[19] In my research the hydrogen bonding is introduced in a copolymer consisting of n-butyl acrylate **14** and the Napy monomer **12**.

Results and discussion

*Reaction 1: Synthesis of the supramolecular star core **4***

The star core was synthesized starting from trimethylol propane triglycidyl ether **1**, which is an easy accessible chemical. The first step of the synthesis is the azidation of the epoxy end group. In the second step, thymine-based hydrogen bonding moieties **3** are introduced by a CuAAC click reaction. A supramolecular polymer structure can be obtained by hydrogen bonding interactions between the thymine units of the star core and diamino triazine units attached to polymer chains.

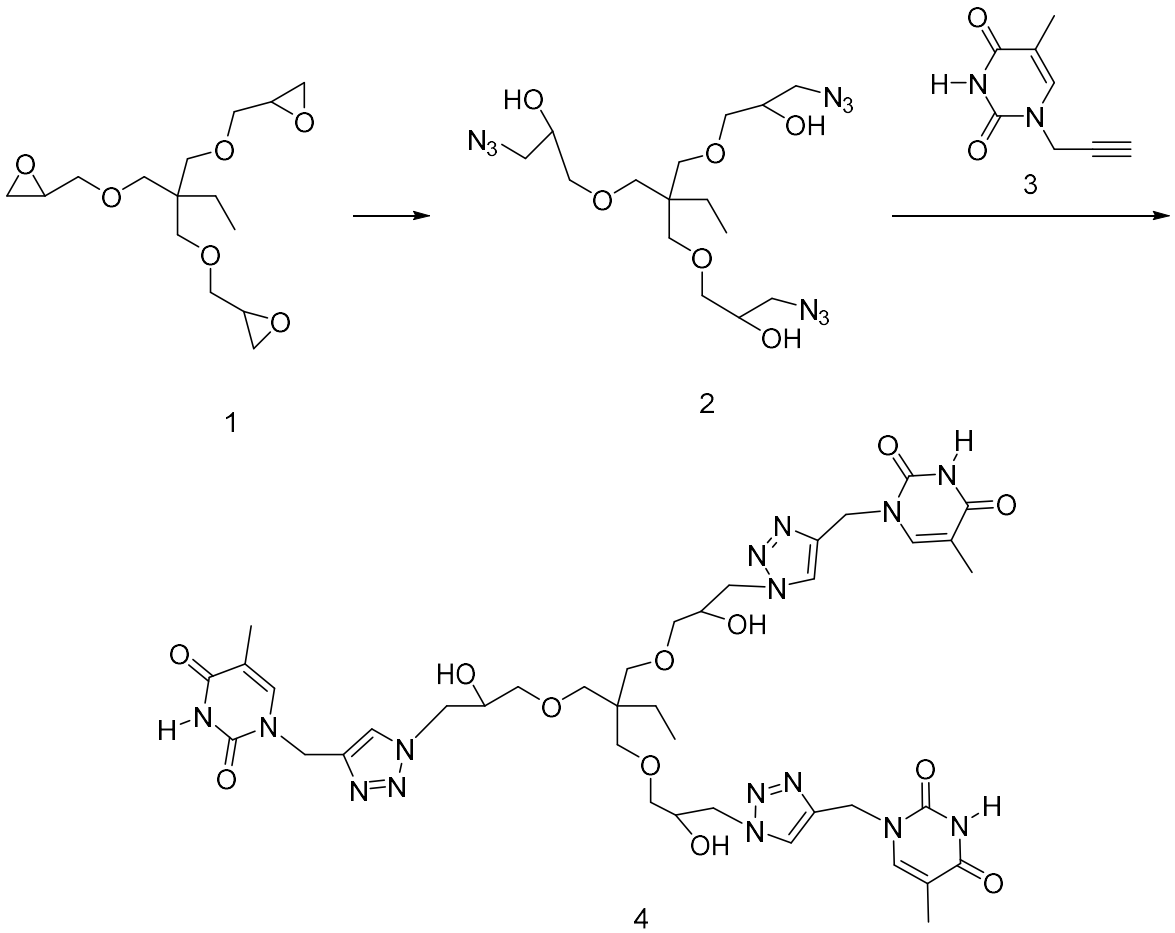

Scheme 8. Synthesis of a supramolecular star core with thymine-based end groups

*Reaction 1.1: Synthesis of trimethylolpropane-1-azidobutan-2-yl-acetate ether **2***

The first step in the synthesis of the supramolecular star core is the azidation of trimethylolpropane triglycidyl ether **1** (scheme 9).[8] In this reaction ammonium chloride is used for the protonation of the formed alkoxide. During the 19 hours lasting reaction, the reaction mixture turned from a white suspension into a slightly yellow suspension. After

extraction with chloroform, product **2** of this reaction was obtained as a yellow viscous liquid with a yield of 58%.

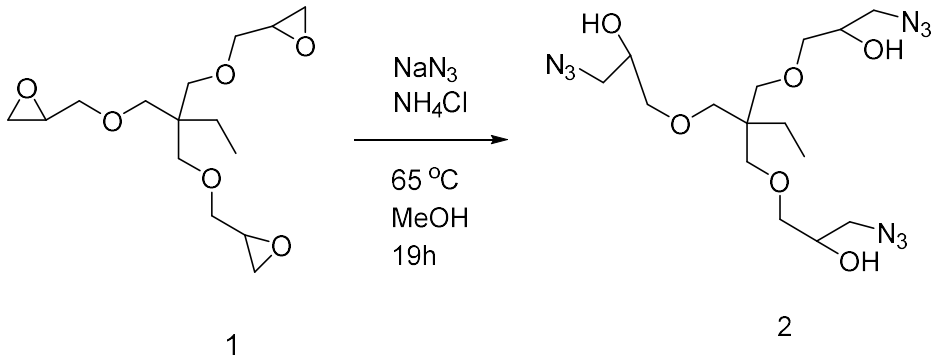

1 2

Scheme 9. Azidation of trimethylolpropane triglycidyl ether **1** to form compound **2**

According to the ^{1}H NMR analysis of compound **2** after the extraction, the product contained only small amounts of methanol and grease (figure 7). Also, the multiplet around 3.48 ppm has a higher integration than expected. From ^{1}H NMR analysis of trimethylolpropane triglycidyl ether **1**, it can be concluded that those impurities were already present in the starting material. This is not a problem, since the impurities will be removed in the purification after the next reaction step.

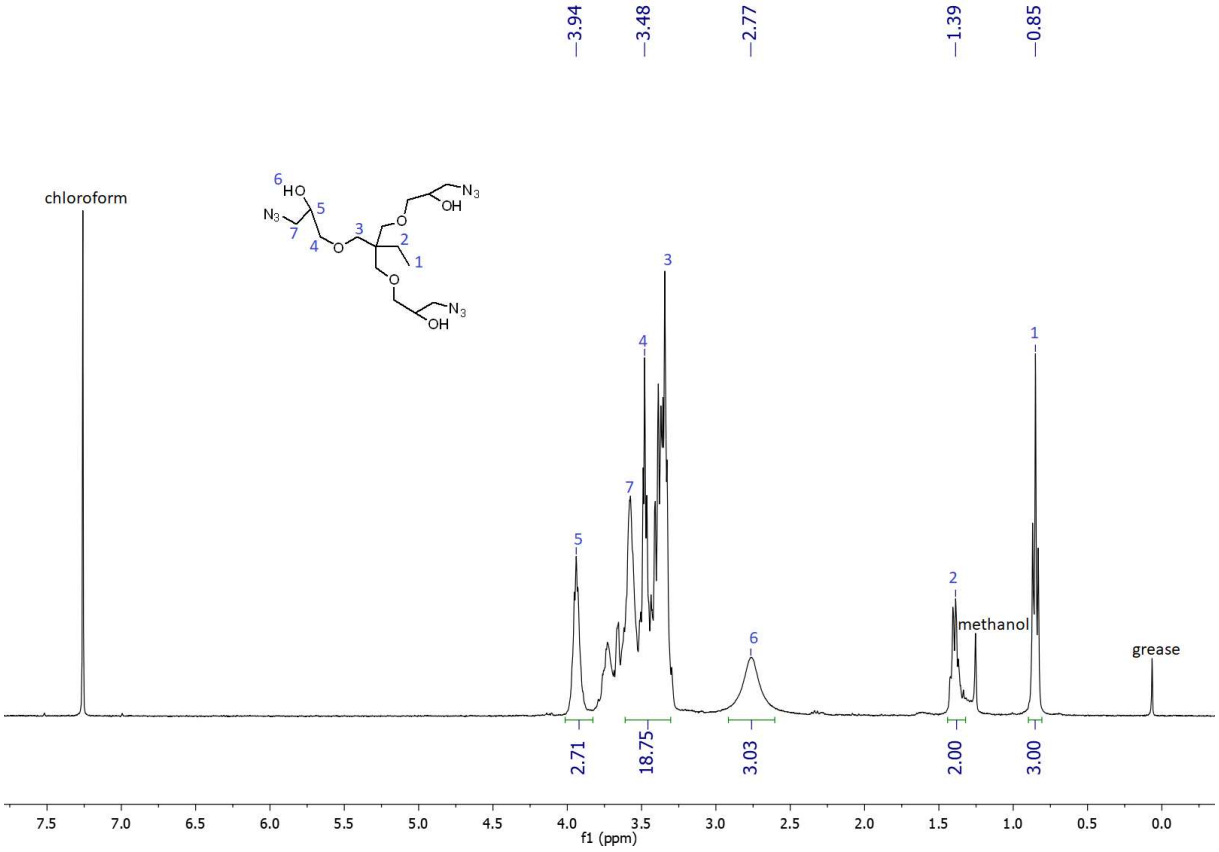

Figure 7. ^{1}H NMR spectrum of compound **2** from reaction 1.1

Reaction 1.2: Click reaction

To introduce the hydrogen bonding moieties **3** based on thymine, the CuAAC click reaction was used (scheme 10). This reaction was chosen because it is stereospecific, requires mild reaction conditions and can be performed in a wide variety of solvents.[11] The azide-alkyne cycloaddition is catalysed by a copper complex which is formed by the reduction of Cu(II) to Cu(I) by sodium ascorbate. During the reaction the formation of the copper complex was visible from the colour of the reaction mixture which changed from green to yellow at the beginning of the reaction.

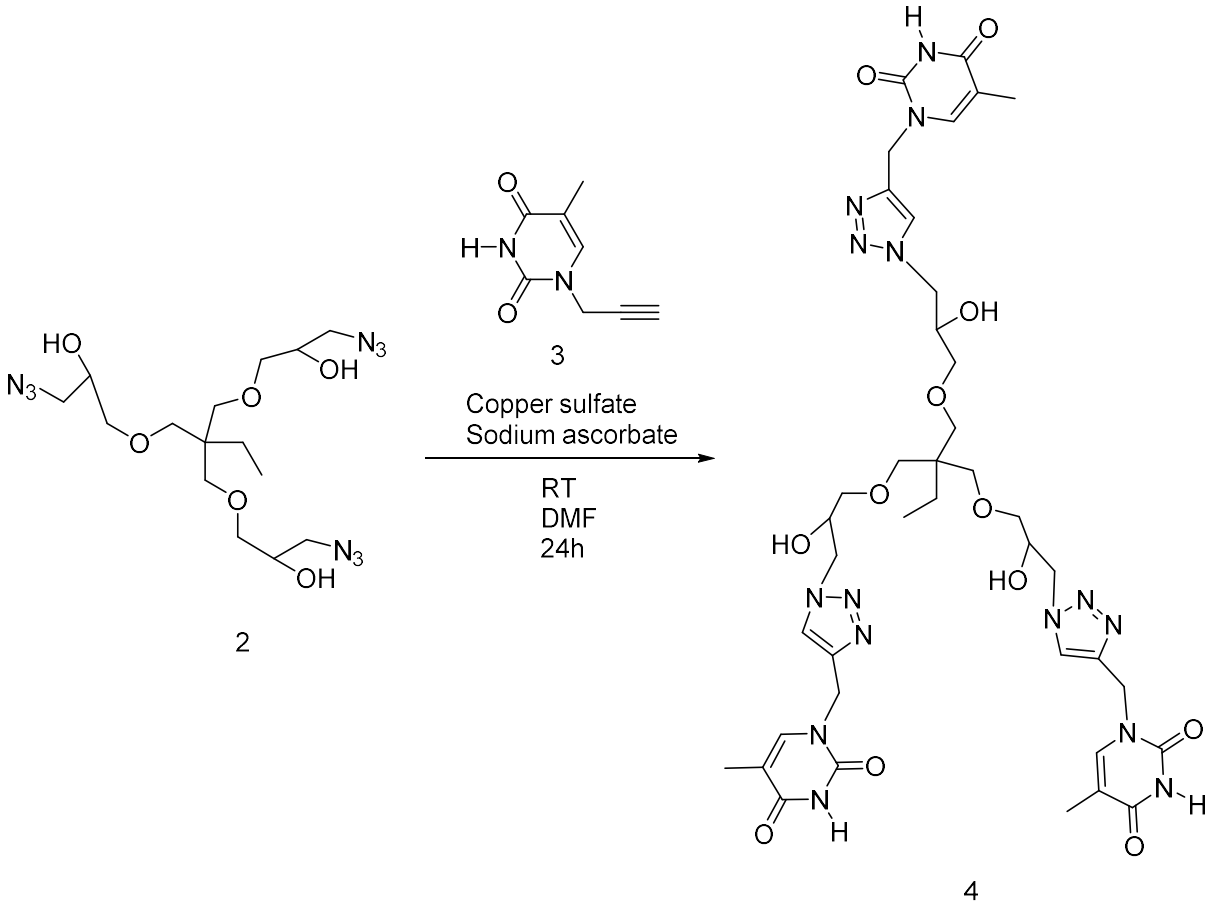

Scheme 10. Click reaction between a trifunctional azide **2** and an alkyne-based sticker **3**

After running the reaction for 24 hours, a ^{1}H NMR sample was taken, resulting the in spectrum of figure 8. After this the reaction mixture was poured into a HCl solution (0.1 M) and the product was extracted with DCM. Followed by drying the organic layer with $MgSO_4$ and concentrating the product mixture.

The ^{1}H NMR spectrum in figure 8 shows next to the thiamine-based sticker **3**, DMF, water and DMSO peaks, the two characteristic peaks for the formation of the triazole ring. H_7 can

be found at 7.58 ppm and corresponds to the triazole proton. H_8 can be found at 4.87 ppm and corresponds to the allylic proton between the triazole ring and the thymine group. H_8 has a higher shift than the proton which can be found at the same position in the thiamine sticker **3**, since the newly formed double bond is less electron donating than the triple bond of the thiamine sticker **3**. Therefore, H_8 is less shielded. From the ratio between H_1 and H_7, a conversion of 53% could be calculated. The low conversion could have been caused by steric hindrance or the short reaction time. The attempt to isolate the product by column chromatography did not succeed, because the polarity of the product mixture was really close to the polarity of the starting materials, therefore several components had similar retardation factors (R_f).

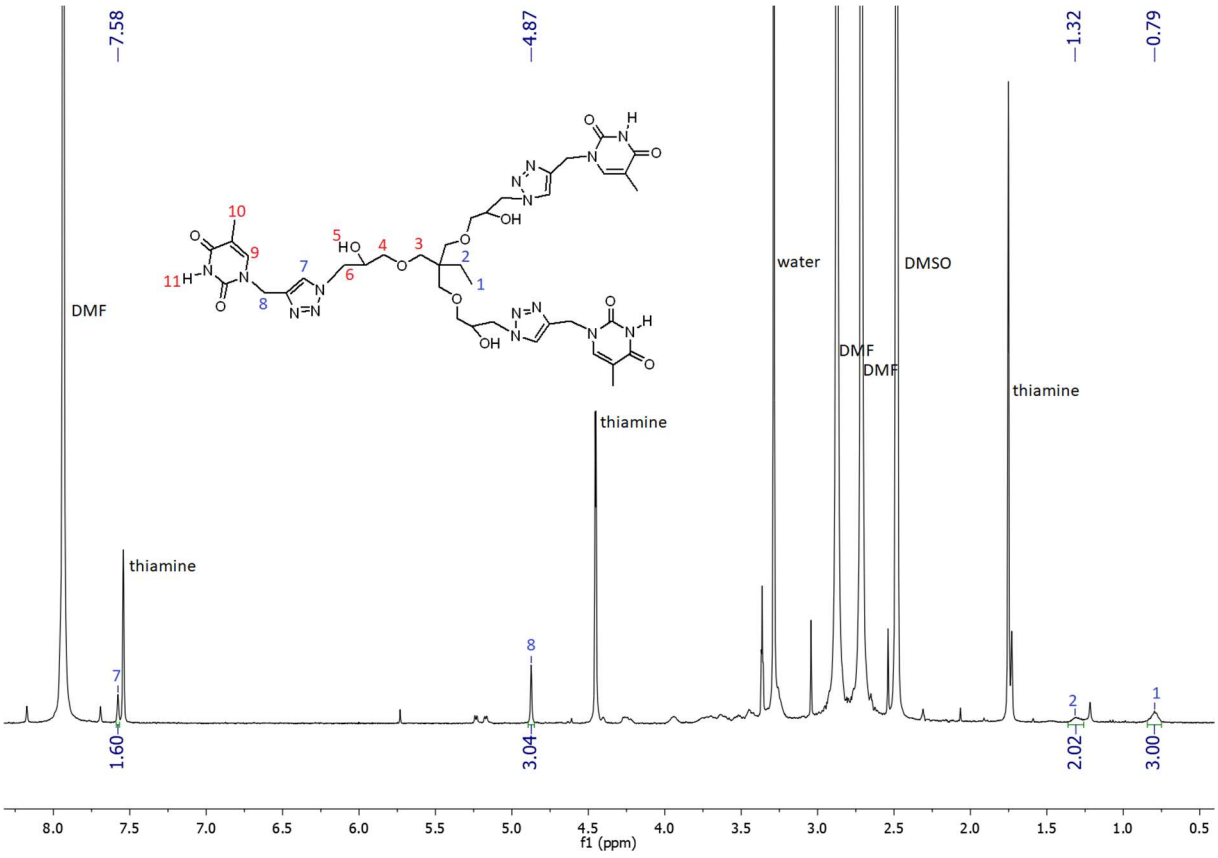

Figure 8. ^{1}H NMR spectrum of the product mixture from reaction 1.2

An improvement for the removal of the excess of the thymine-based sticker could be the use of alkyne magnetic beads. After the reaction the beads can be added to the reaction mixture. After all the thymine-based sticker is attached to the beads, it can be washed out very easily.[20] But since there was no access to more thiamine-based sticker **3** and the synthesis of the compound takes a lot of time, I moved on to the synthesis of another supramolecular architecture, which is explained in the next chapters.

*Reaction 2: Synthesis of monomer with Napy monomer **12***

Monomer **12** with a hydrogen bonding moiety based on Napy was synthesized starting from 2,6-amino pyridine **6** and DL-malic acid **7**, forming compound **8**. In the second step, HDI **9** was added to introduce an alkyl spacer and to increase the hydrogen bonding capacity of the monomer. Finally, 2-hydroxyethyl acrylate **11** was added to introduce the reactive double bond where the polymerization can start from (scheme 11).

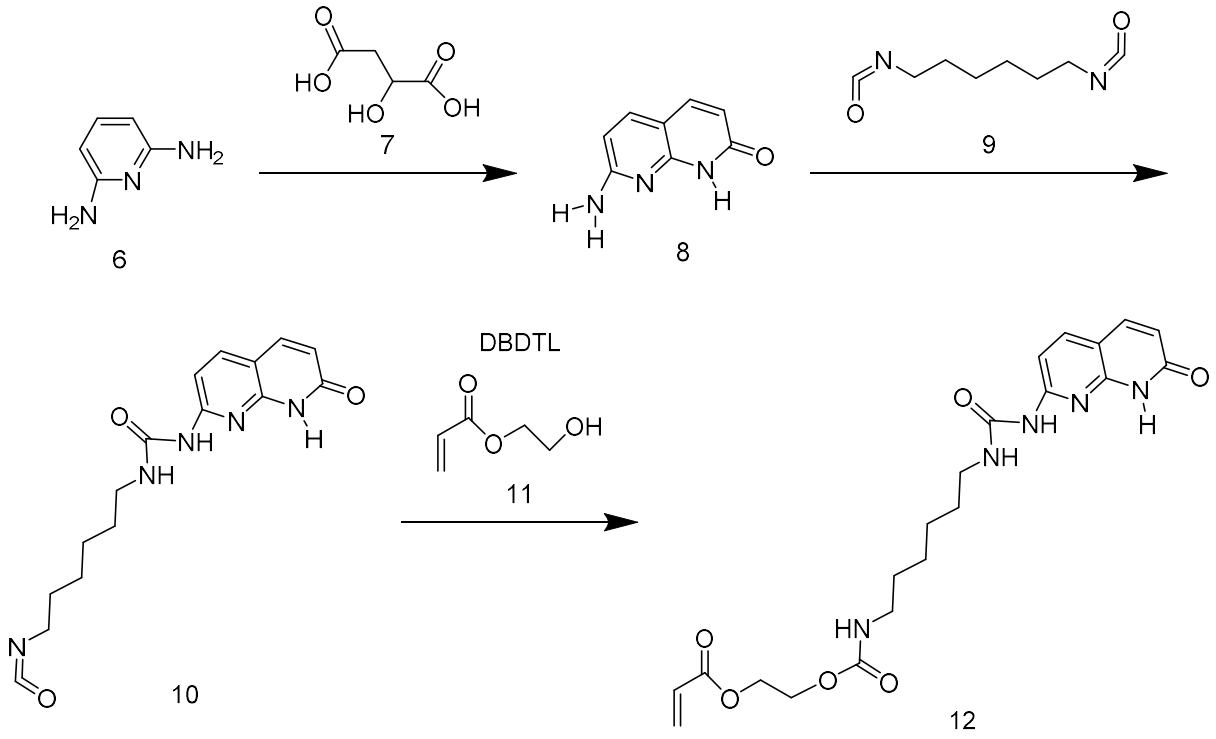

Scheme 11. Synthetic route for the Napy-based monomer **12**

Reaction 2.1: Synthesis of 7-amino-1,8-naphthyridin-2(1H)-one

The first step in the synthesis of monomer **12**, is the reaction between 2,6-amino pyridine **6** and DL-malic acid **7** (scheme 12). After mixing the two compounds by grinding, concentrated sulfuric acid (97%) was added dropwise at 0 °C, subsequently the reaction was heated to 110 °C for 3.5 hours. During the reaction the brown suspension has changed to an almost black solution upon the release of gas, which indicated the release of carbon dioxide. The reaction was quenched by adding a solution of ammonium chloride (27%) dropwise at 0 °C until a pH of 9. This resulted in the precipitation of a light brown solid. Compound **8** was obtained quantitative and was directly used for the next step.

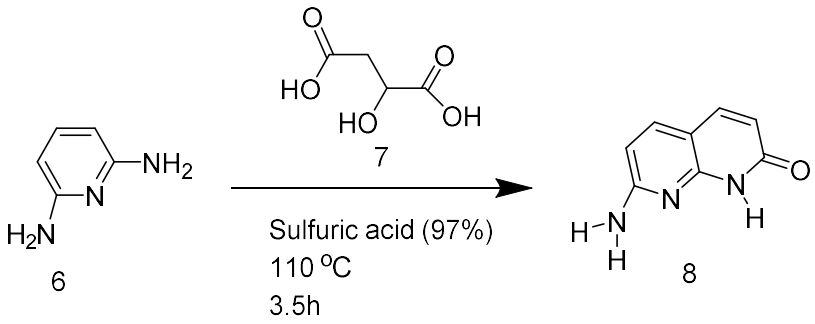

Scheme 12. Synthesis of 7-amino-1,8-naphthyridin-2(1H)-one **8**

From the ^{1}H NMR spectrum of compound **8** it can be concluded that the product was obtained pure (figure 9), therefore it could be directly used for the next reaction step without any additional purification.

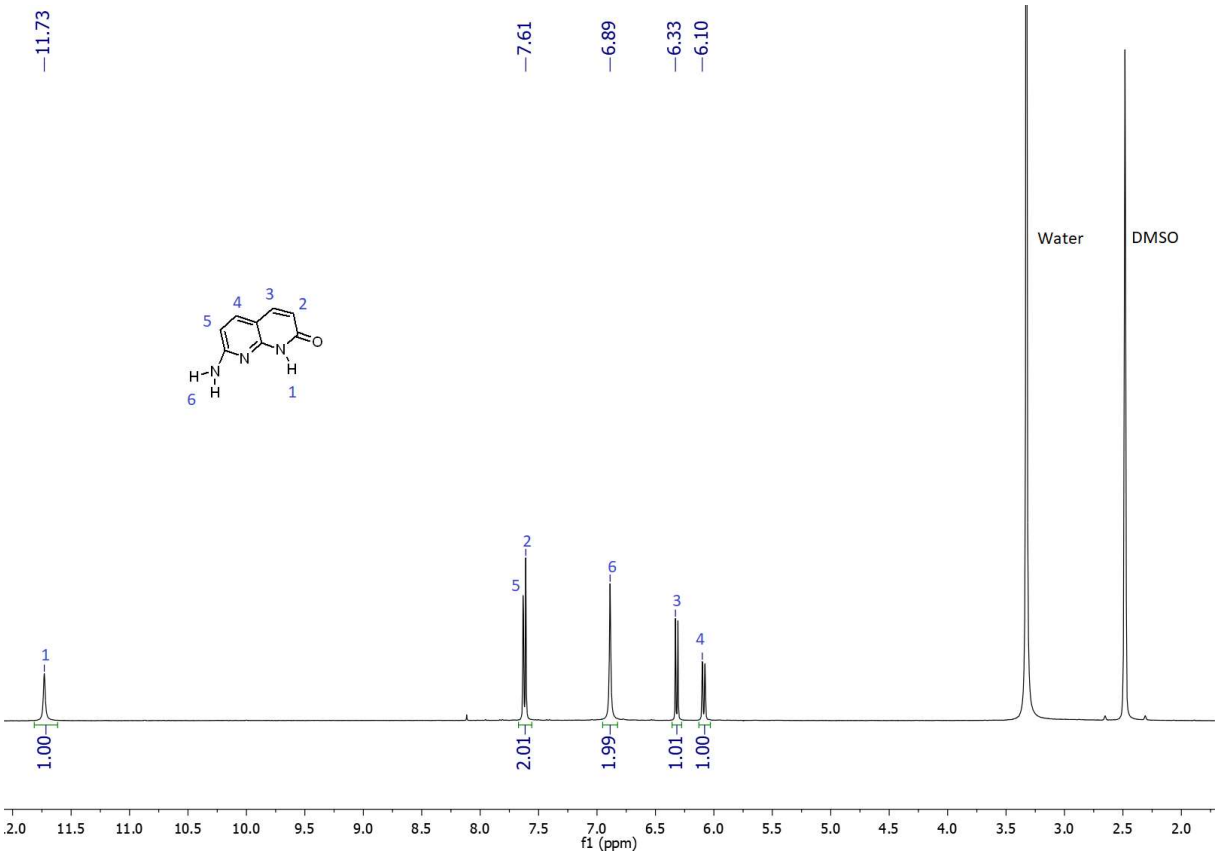

Figure 9. ^{1}H NMR spectrum of compound **8**

*Reaction 2.2: Synthesis of 1-(6-isocyanatohexyl)-3-(7-oxo-7,8-dihydro-1,8-naphthyridin-2-yl)urea **10***

For the second step in the synthesis of the monomer **12**, compound **8** was dried for 1 hour at 110 °C under vacuum. After the addition of a large excess HDI **9** (about 14 equivalents) to compound **8**, the reaction mixture was allowed to stir for 19 hours at 110 °C. During the reaction, the light brown compound **10** precipitated (scheme 13). The reaction was stopped

by cooling down and precipitation in n-hexane. After filtration, the remaining n-hexane was removed overnight in a vacuum oven at 40 °C.

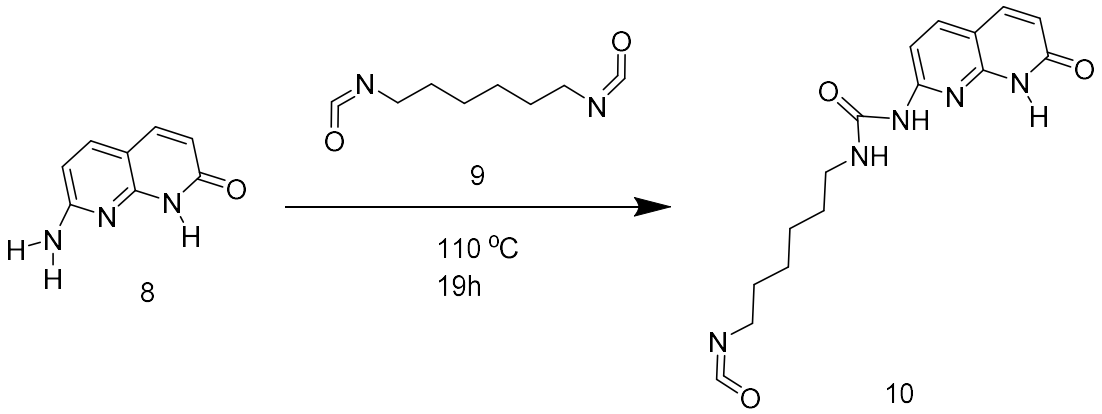

Scheme 13. Synthesis of 1-(6-isocyanatohexyl)-3-(7-oxo-7,8-dihydro-1,8-naphthyridin-2-yl)urea **10**

During the first attempt to synthesize compound **12**, the dried compound **10** was directly used as starting compound for the next step. This resulted in a mixture of side products that consisted mainly of a compound formed from the reaction between HDI **9** and 2-hydroxyethyl acrylate **11**, which means that still a lot of HDI **9** was present after the purification of the previous reaction step. To avoid this, the product from the second step should be distilled prior to use. Most HDI **9** was removed under vacuum at 130 °C.

From the ^{1}H NMR spectrum of compound **10** it can be seen that the product still contains some HDI **9**, since the multiplet around 1.33 ppm has a higher integration than 8 (figure 10). But this is not problematic since in the next step an excess 2-hydroxyethyl acrylate **11** is used.

During ^{1}H NMR analysis, M. Golkaram observed that compound **10** forms different tautomers in DMSO. The main tautomer in DMSO has internal hydrogen bonding between H_7 and the nitrogen of the pyridine ring. The small peaks that appear in the spectrum between 6.0 ppm and 12.0 ppm in figure 10 are caused by other tautomers.

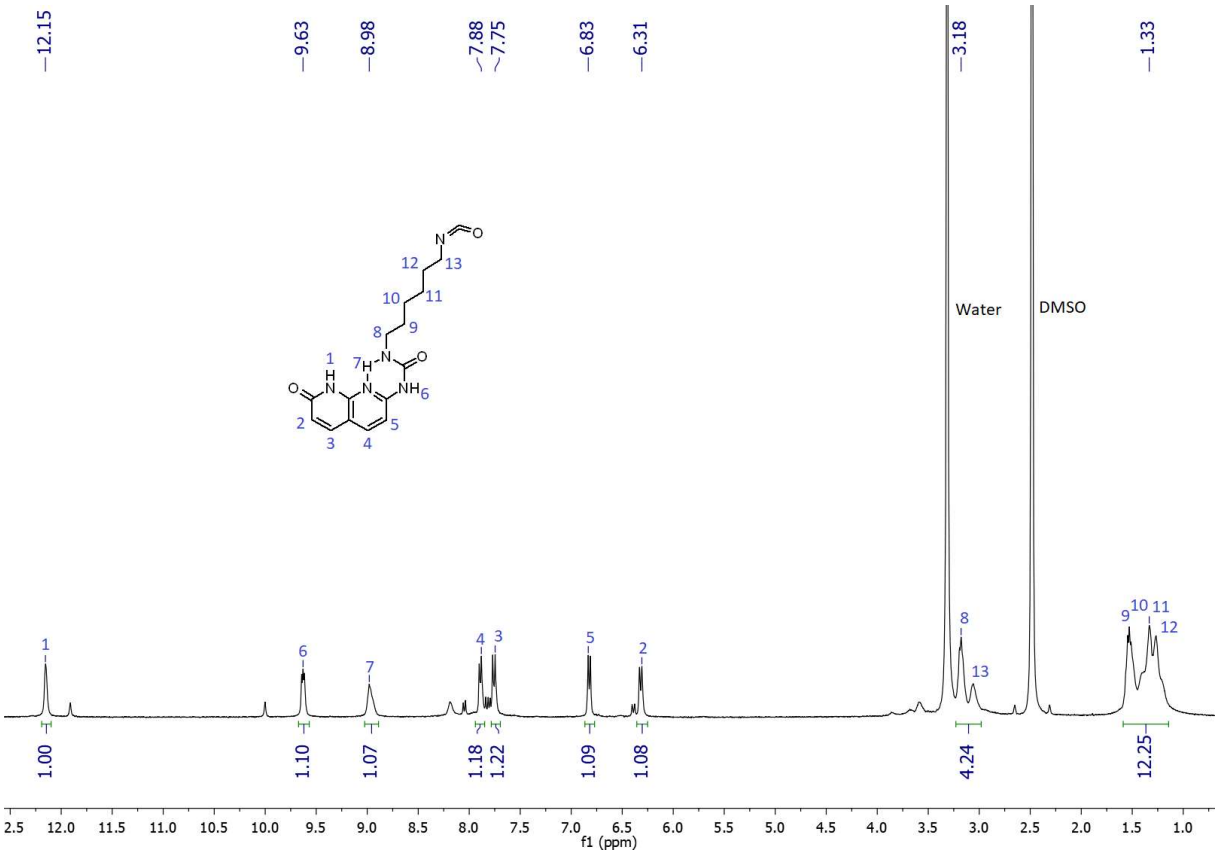

Figure 10. ^{1}H NMR spectrum of product 10

*Reaction 2.3: Synthesis of 2-(((6-(3-(7-oxo-7,8-dihydro-1,8-naphthyridin-2-yl)ureido)hexyl)carbamoyl)oxy)ethyl acrylate **12***

For the final step of the synthesis of the monomer, compound **10** was first grinded to powder. DBDTL was used as catalyst for the reaction between compound **10** and 2-hydroxyethyl acrylate **11** (about 4.5 equivalents) (scheme 14). Since compound **10** is not perfectly soluble in chloroform (even at reflux a suspension is observed), it is not fully converted to compound **12**.

After the reaction, the mixture is precipitated in n-hexane. To remove the remaining starting compounds, the product mixture is dissolved in DCM and washed with water and brine. Because the product is partly hydrophilic and partly hydrophobic, an extra layer was formed between the aqueous layer and the organic layer. Also, a precipitate was formed. Due to these inconveniences, a lot of product was lost during the work-up (yield = 42 %).

To reduce the amount of product lost during the work-up, the product mixture was dissolved in DMSO and precipitated in water instead of performing an extraction. By doing this, all 2-hydroxyethyl acrylate **11** was removed.

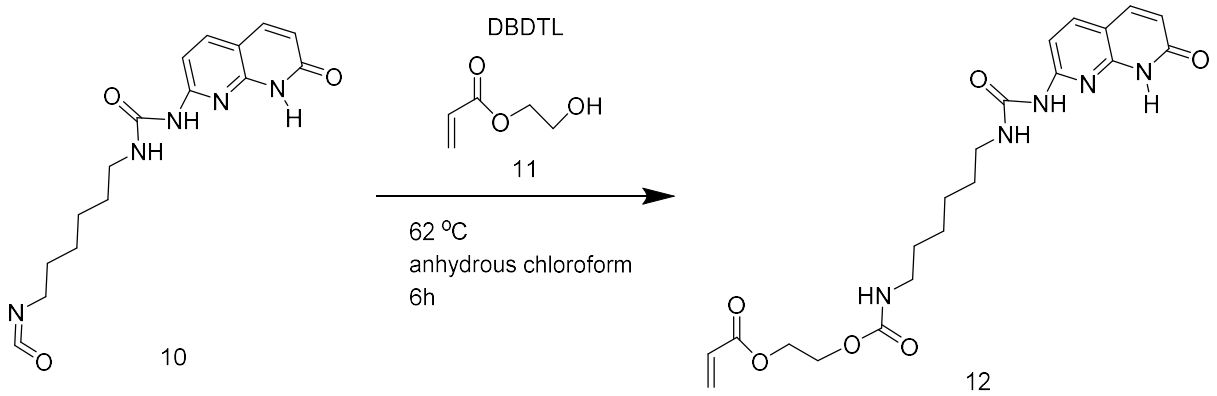

Scheme 14. Synthesis of 2-(((6-(3-(7-oxo-7,8-dihydro-1,8-naphthyridin-2-yl)ureido)hexyl)carbamoyl)oxy)ethyl acrylate **12**

Since the characteristic product peak, H_{14}, is visible in the ^1H NMR spectrum with an integration similar to proton H_2, H_3 and H_4 we can conclude that compound **12** is obtained pure (figure 11).

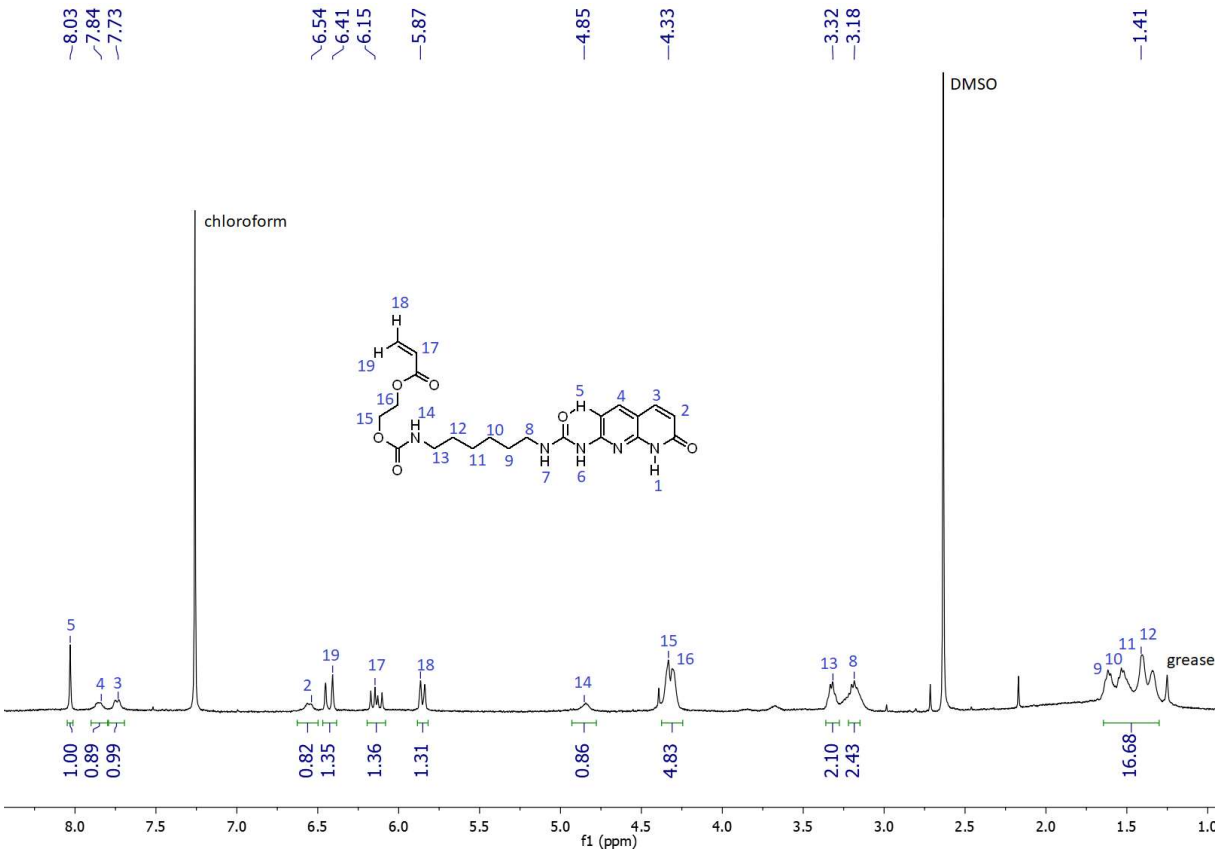

Figure 11. ^1H NMR spectrum of product 12

Product **12** forms different tautomers in both chloroform and DMSO. In chloroform the only tautomer that is formed has hydrogen bonding between H_5 and the closest ketone. Due to this hydrogen bonding interaction, electron density is withdrawn from H_5. Therefore, the proton is deshielded and the corresponding peak moves to the left of the spectrum (figure 12).

In DMSO two or more tautomers are formed from which the main tautomer has hydrogen bonding between H_7 and the lone pair of the nitrogen in the pyridine ring, resulting in deshielding of H_7 and shifting the corresponding peak to the left of the spectrum (figure 12). Since in DMSO also other tautomers are formed, several small peaks are visible in the ^1H NMR spectra. Also, this can result in the product peaks to have a lower integration than expected.

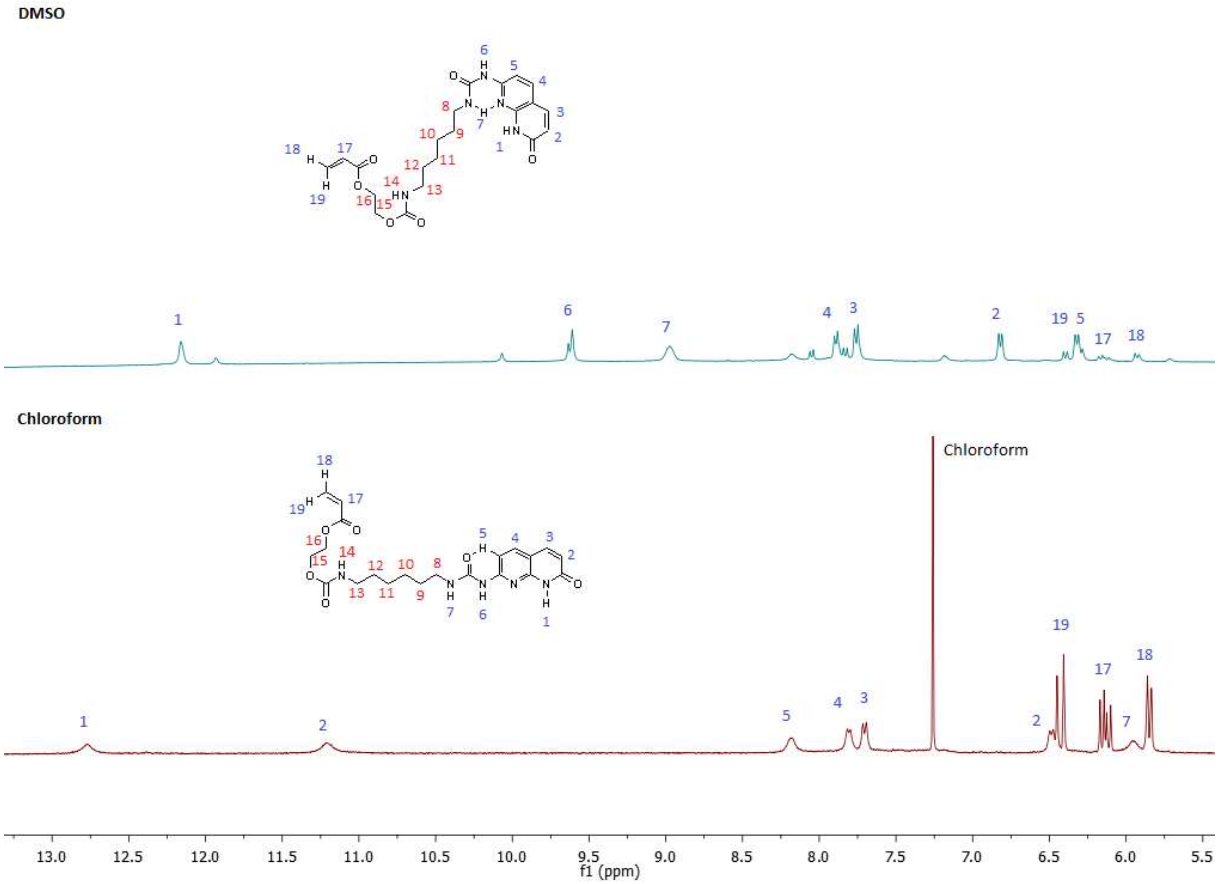

Figure 12. Tautomers formed of product 12 in chloroform and DMSO

It is also expected that in chloroform compound **12** forms dimers as is indicated in figure 13. The formation of dimers for the main tautomer in DMSO is not possible, since internal hydrogen bonding between H_7 and the lone pair of the nitrogen in the pyridine ring, results in a geometry change that doesn't allow the formation of dimers.

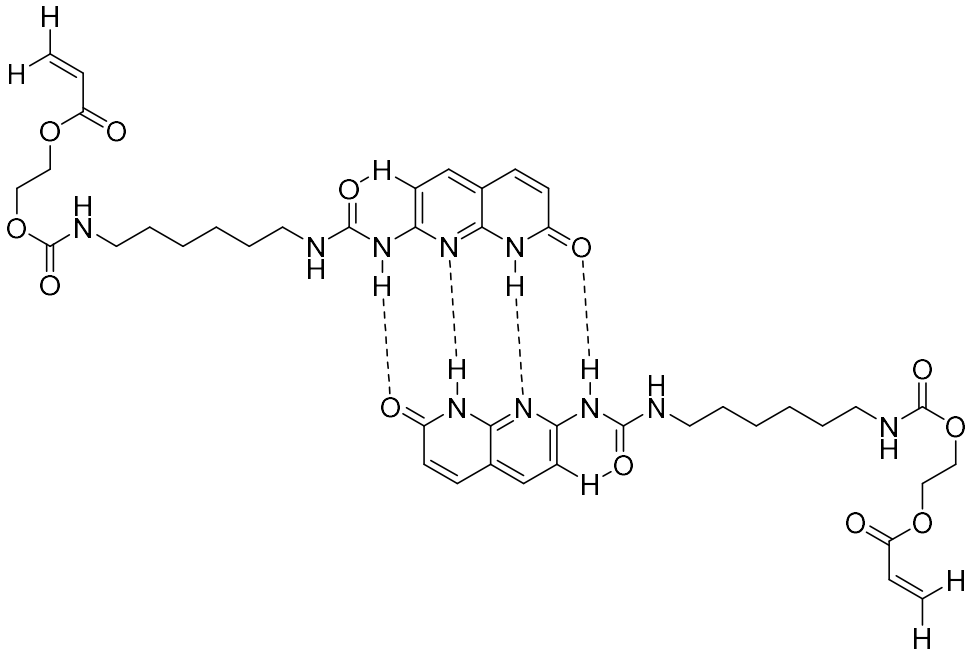

Figure 13. Formation of dimers of compound **12** in chloroform

*Reaction 3.1: Raft polymerization of 2-(((6-(3-(7-oxo-7,8-dihydro-1,8-naphthyridin-2-yl)ureido)hexyl)carbamoyl)oxy)ethyl acrylate **12***

Monomer **12** was polymerized by a RAFT polymerization in DMSO. AIBN was used as initiator and DBTTC was used as chain transfer agent.

To test if the circumstances work for the synthesized monomer, first a polymerization with a monomer similar in structure was done. In this case n-butyl acrylate was used since it is cheap and easy accessible. GPC was used to determine the PDI and molecular weights. The molecular weights of poly (n-butyl acrylate) showed that the radical polymerization for n-butyl acrylate worked. However, the PDI's were a bit high with values around 1.5. This might be a result of the side reactions occurring at high conversions during RAFT polymerization, such as chain transfer and coupling reactions. Therefore, the Raft polymerization of compound **12** was run for 6h instead of the 19h for the polymerization of n-butyl acrylate.

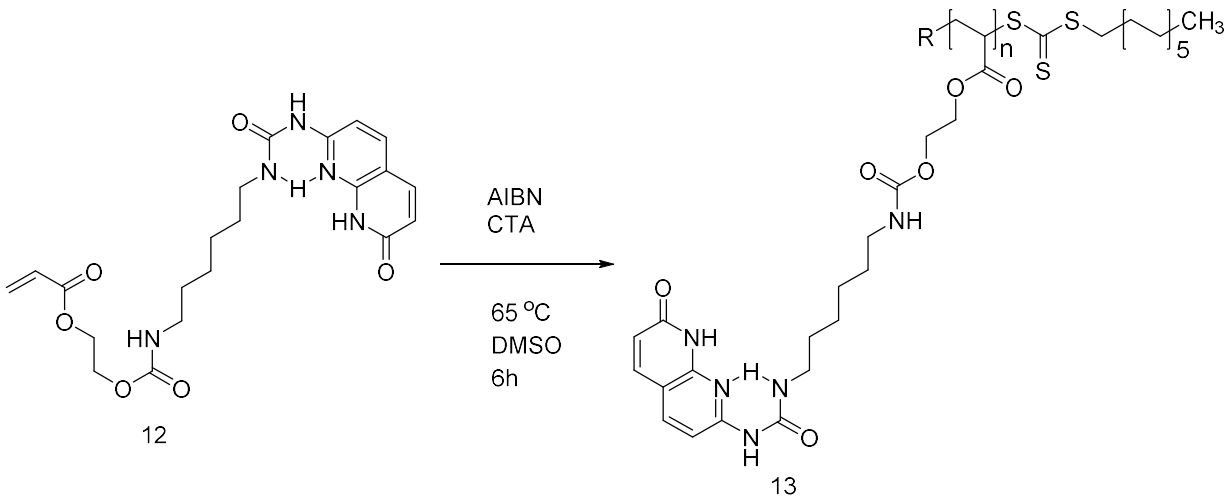

Scheme 15. RAFT polymerization of 2-(((6-(3-(7-oxo-7,8-dihydro-1,8-naphthyridin-2-yl)ureido)hexyl)carbamoyl)oxy)ethyl acrylate **12**

The same circumstances as for the polymerization of n-butyl acrylate where applied for the polymerization of the monomer **12**. But this time, DMSO was used as solvent instead of DMF. After precipitation in methanol, polymer **13** was obtained as a dark brown solid. Due to the poor solubility in THF and DMF no GPC measurements were performed. Although the polymer is soluble in DMSO, it could not be used for GPC measurements, since the column was defect. Also, MALDI-ToF MS didn't give any results due to poor solubility of the polymer. From ^{1}H NMR analysis it can be concluded that the monomer has polymerized, since the vinylic hydrogens between 5.50 ppm and 6.25 ppm of monomer **12** have almost disappeared (figure 14). However, the average molecular weight $\overline{M_n}$ could not be calculated, since the peaks for the aromatic end group of DBTTC are overlapped by the peaks for product. Therefore, the polymerization was carried out with the chain transfer agent DDMAT which results in peak H_{17} at 0.81 ppm for the methyl end group. From the ratio between the end group protons H_{17} and the aromatic proton H_5, the average molecular weight of $\overline{M_n}$ = 4,050 g/mol was calculated. This is close to the aimed molecular weight $\overline{M_n}$ = 5,000 g/mol where the amounts of initiator and CTA were calculated for. However, since the H_{17} is located on the hill of the multiplet around 1.27 ppm, the actual integration is expected to be lower. This means that the average molecular weight is probably higher than $\overline{M_n}$ = 4,050 g/mol.

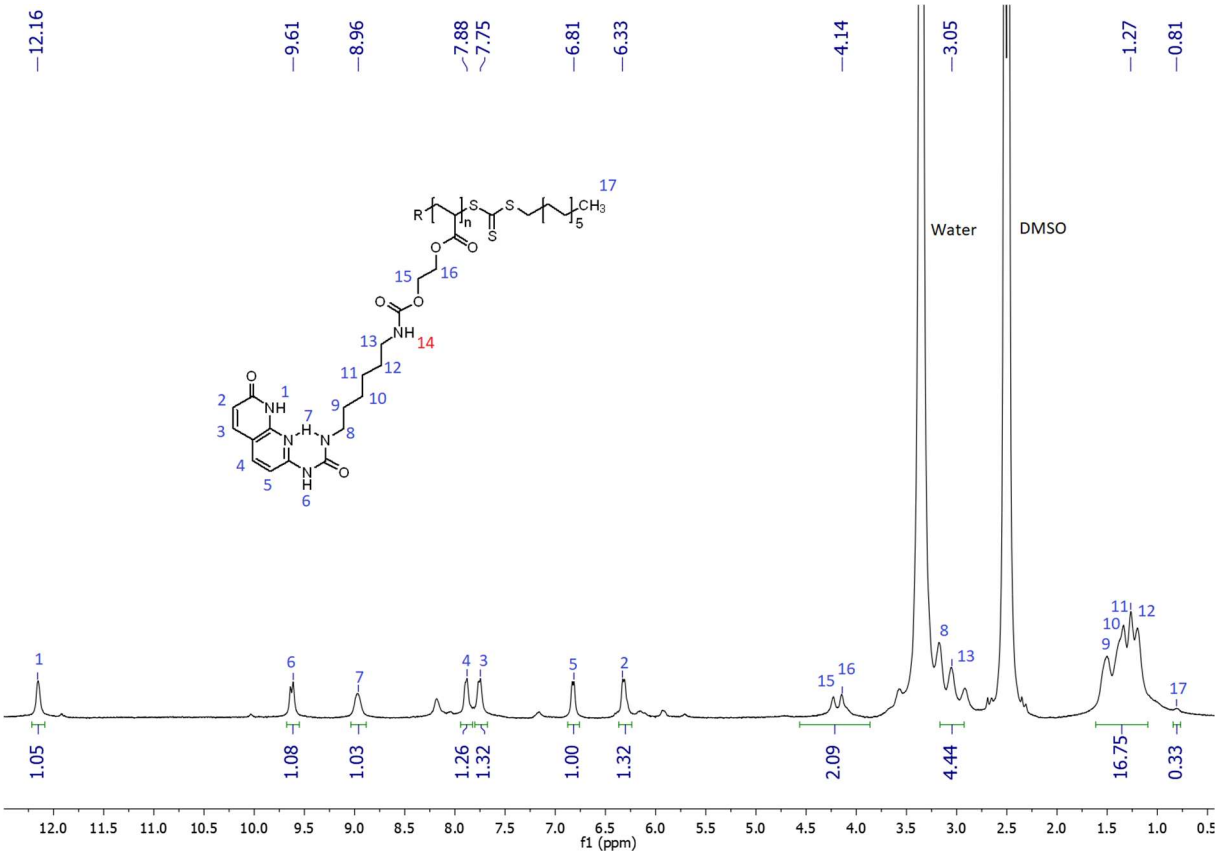

Figure 14. ^{1}H NMR spectrum of poly polymer **13**

To determine the decomposition temperature of the formed polymer, TGA was performed. From the graph in figure s3 it can be seen that at 93.0 °C the remaining solvent was evaporated, resulting in a weight loss of 4.3 %. The thermal decomposition temperature ($T_{d(max)}$) can be found 238.4 °C resulting in a weight percentage loss of 45.5 % (figure 15).

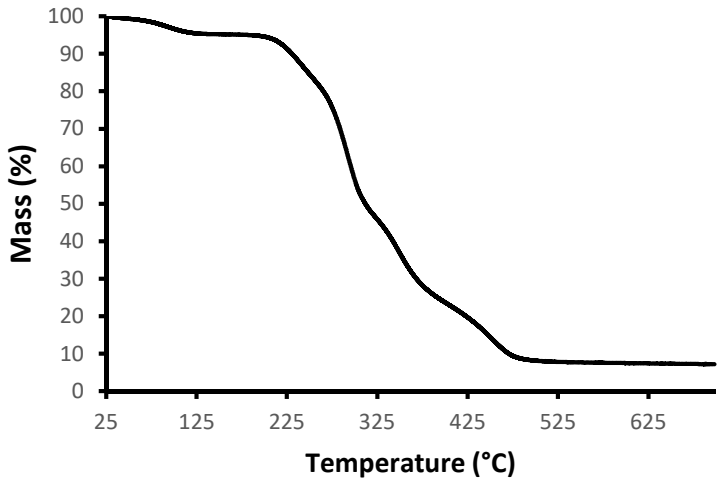

Figure 15. TGA analysis of polymer **13** with $\overline{M_n}$ = 4,050 g/mol

Several DSC measurements were performed to determine the T_g of the polymers synthesized from monomer **12**. Since no peaks are observed in the DSC spectra before degradation occurred, it is assumed that the T_g of the polymer is close to or higher than the degradation temperature of 238.4 °C. The DSC spectrum with the first heating scan and the corresponding cooling scan is depicted in figure 16.

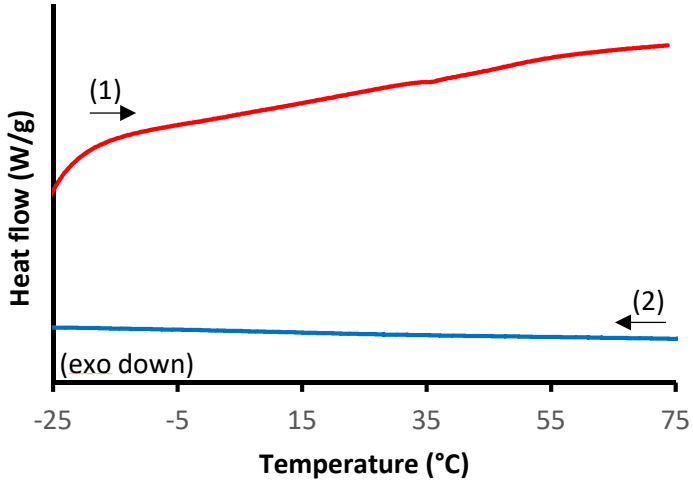

Figure 16. DSC analysis of polymer **13** with $\overline{M_n}$ = 4,050 g/mol

*Reaction 3.2: Copolymerization of n-butyl acrylate and 2-(((6-(3-(7-oxo-7,8-dihydro-1,8-naphthyridin-2-yl)ureido)hexyl)carbamoyl)oxy)ethyl acrylate **12***

A copolymer with an aimed degree of polymerization (X_n) of 300 was synthesized starting from different feed compositions of Napy monomer **12** and n-butyl acrylate **14**. AIBN and DBTTC were used as initiator and CTA respectively. Before the polymerization, n-butyl acrylate was purified by a basic aluminium oxide column to remove the inhibitor. After mixing the components in DMSO, a yellow suspension was visible. For the copolymerization it was assumed that monomer **12** and n-butyl acrylate **14** have the same reactivity and therefore the product is expected to be a random copolymer having the same composition as the monomer feed. The mole percentage of monomer **12** ($X_{\text{monomer 12}}$) in the copolymer determined by ^{1}H NMR analysis and compared to the monomer feed ratio (table 1).

Monomer 12 feed	$X_{monomer\ 12}$	T_g	$T_{d(max)}$
mole %	mole %	°C	°C
0	0	-49.2	/
1	1	-48.9	396.9
3	3	-46.9	401.1
10	7	-42.8	399.3
30	34	27.5	311.7

Table 1. Mole fractions of the Napy monomer **12** in the copolymer with corresponding T_g and $T_{d(max)}$

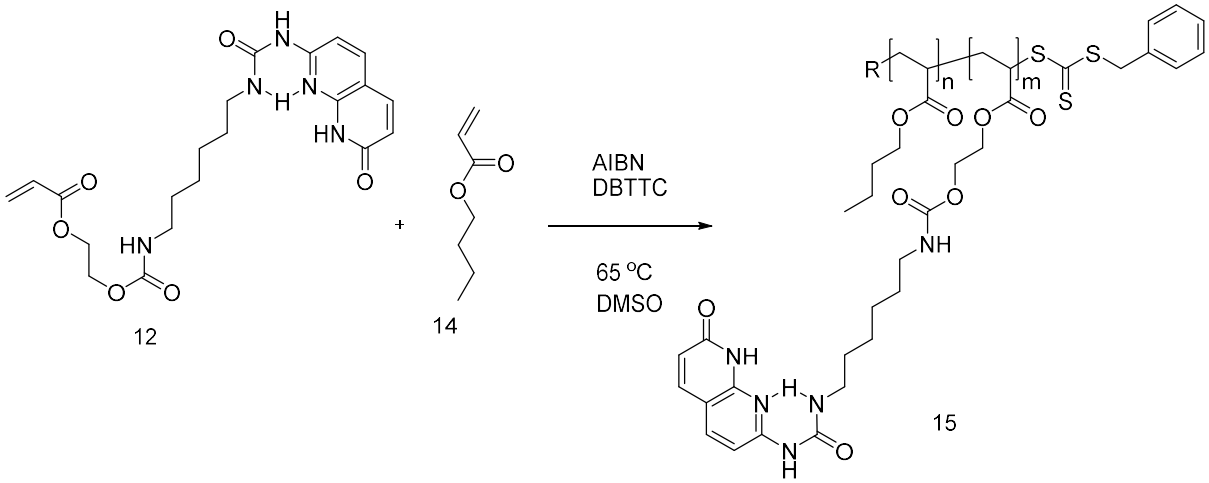

Scheme 16. Copolymerization of Napy monomer **12** and n-butyl acrylate **14**

^{1}H NMR analysis was performed to calculate the fraction of both monomers in the polymer (figure 17). The composition ($X_{monomer\ 12}$) was calculated from the ratio between the multiplet around 1.33 ppm and a monomer **12** peak (in this case H_5). Although this method gives relatively good results in this study, it is not perfectly reliable since impurities and solvent residues can result in a larger integration of the multiplet around 1.33 ppm. Therefore, the information in table 1 should be used with care.

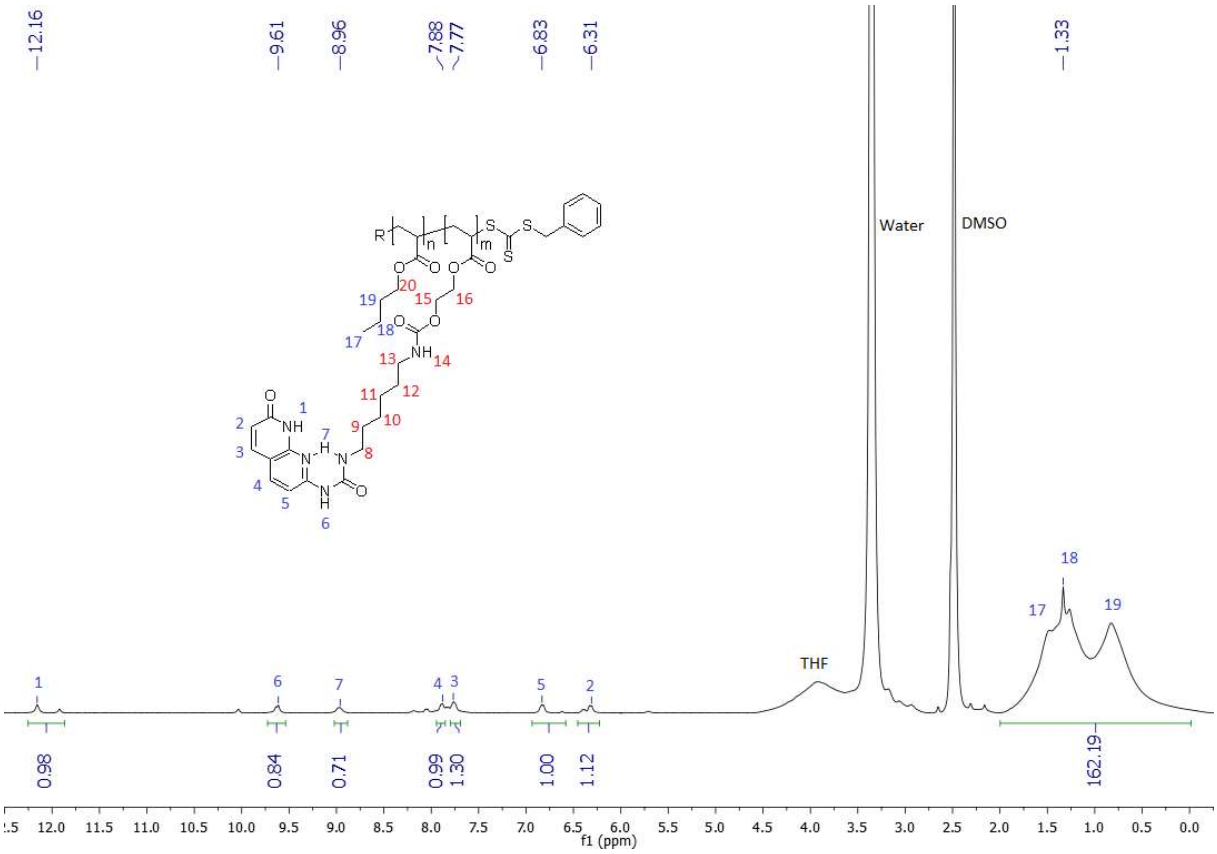

Figure 17. ^{1}H NMR spectrum of polymer **15** with a monomer feed of 10% compound **12** and 90% compound **14**

From table 1 it can be seen that the copolymers sometimes have a higher or lower Napy monomer **12** composition than the corresponding monomer feed. One explanation for this could be the solubility of the copolymer in DMSO. At higher compositions of monomer **12**, the copolymer was soluble in DMSO, but at low compositions it wasn't. Therefore, this could have affected the reactivity of the growing polymer chains resulting in deviation of the compositions. Also, impurities in the ^{1}H NMR sample could have resulted in a different ratio of the peaks in the spectrum, resulting in a different calculated $X_{\text{monomer 12}}$.

The thermal properties of the copolymer with different composition were measured with DSC and were compared to poly (n-butyl acrylate) which is indicated as 0 % Napy (figure 18).

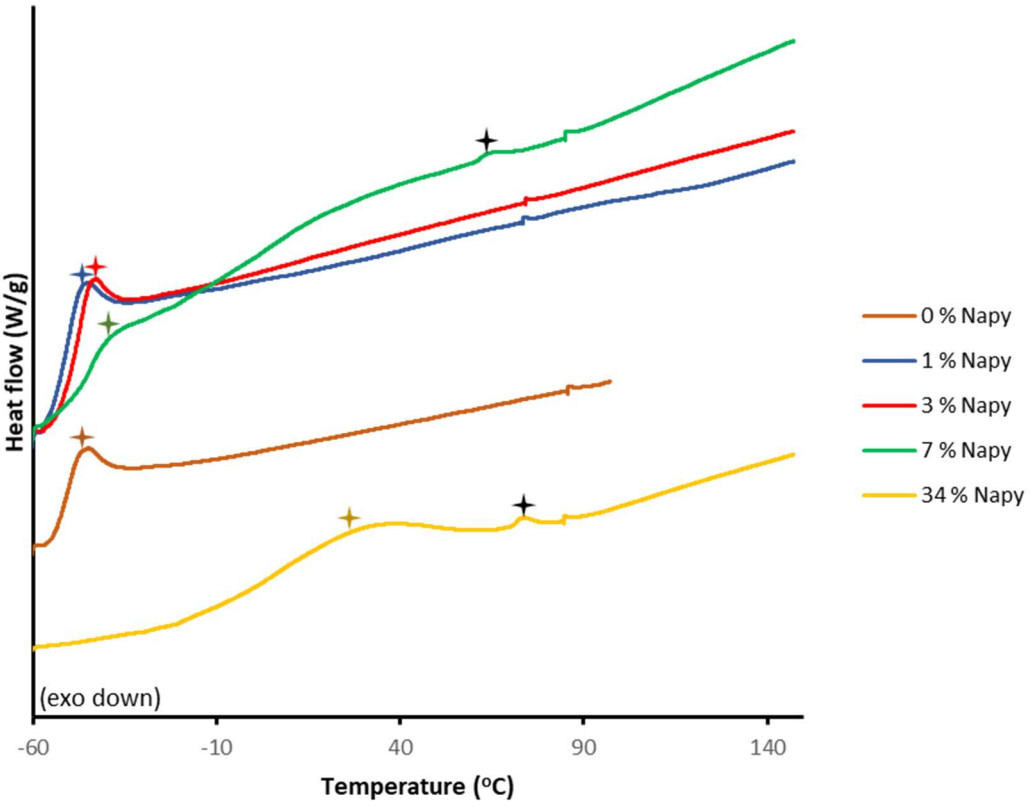

Figure 18. DSC measurements for different compositions of copolymer **15**

From figure 18, it can be seen that the T_g (indicated with the coloured stars) increases with increasing amounts of Napy in the copolymer. This trend can easily be explained by the increasing hydrogen bonding interactions with higher amounts of Napy. However, the copolymers with 7 % and 34 % Napy show two transition temperatures.

The existence of the two different transition temperatures can be explained by the presence of different domains in the polymer melt, which are a result from phase separation. The first transition temperature (indicated with coloured stars) corresponds to the domains with a high n-butyl acrylate concentration and have therefore a transition temperature closer to poly (n-butyl acrylate). The second transition temperature (indicated with black stars) corresponds to the domains with a high Napy concentration and has a higher transition temperature because of strong hydrogen bonding interactions.

Also, just after 75 °C a small peak is visible in all of graphs in figure 18. Since poly (n-butyl acrylate) only has one T_g according to literature, this peak must be a small artefact of the machine.[19]

To get a clear view on how the thermal properties of the Napy copolymer relate to other hydrogen bonding copolymers, the T_g values of the Napy copolymer were compared to the UPy copolymer, which has already been studied.[19]

From figure 19 it can be seen that at low compositions of the hydrogen bonding monomer (X_{HB}) UPy has higher T_g values than Napy, which could indicate that UPy has stronger self-complementary interactions. But since the data from the UPy copolymers is retrieved from another research, and therefore another DSC meter is used, no clear conclusions can be

made. Also, for future research, it is advisable to measure more compositions of the Napy copolymer, to confirm the trends seen in figure 19.

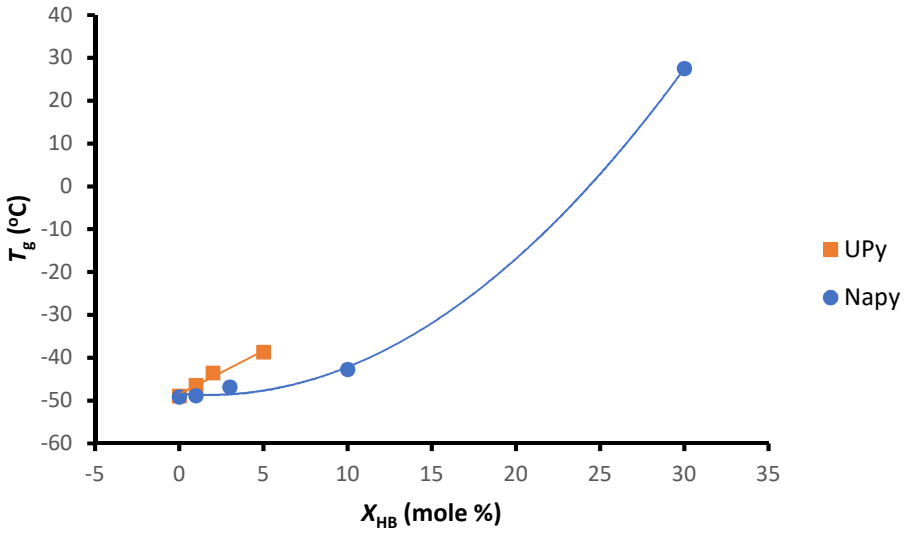

Figure 19. T_g versus different compositions of hydrogen bonding groups in a copolymer of n-butyl acrylate

During rheology measurements also two transition temperatures were observed for the copolymer with 7 % Napy (figure 20). The remarkable observation was made that even after the second transition temperature of around 150 °C the polymer did not flow. From this it can be concluded that even with a mole percent of 7 % Napy monomer **12** in de copolymer, the hydrogen bonding interactions are so strong that the polymer only starts to flow around 300 °C. In future research the rheological properties of the different copolymer compositions will be studied in detail by M. Golkaram.

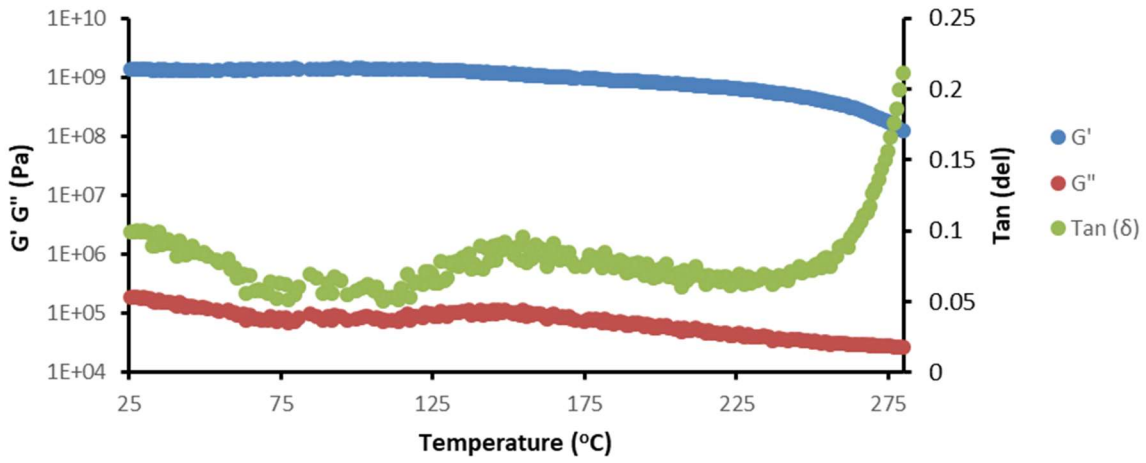

Figure 20. Melt rheology of a copolymer from 7 % Napy monomer **12** and n-butyl acrylate

TGA was performed to determine the $T_{d(max)}$ of the different copolymers of n-butyl acrylate **14** and Napy monomer **12**. From the graphs in figure 21 and the results in table 1 it can be seen that all copolymers have a decomposition temperature around 400 °C, except the copolymer containing 34 % Napy. This could be caused by the high Napy monomer **12** content, since 34 % copolymer has a $T_{d(max)}$ which is in between the $T_{d(max)}$ of 238.4 °C of the Napy homopolymer **13** and the copolymers with low Napy concentrations. The graphs of the copolymer containing 1 % Napy and 34 % Napy already show weight loss around 100 °C, this is caused by the evaporation of the water which was still present in the sample.

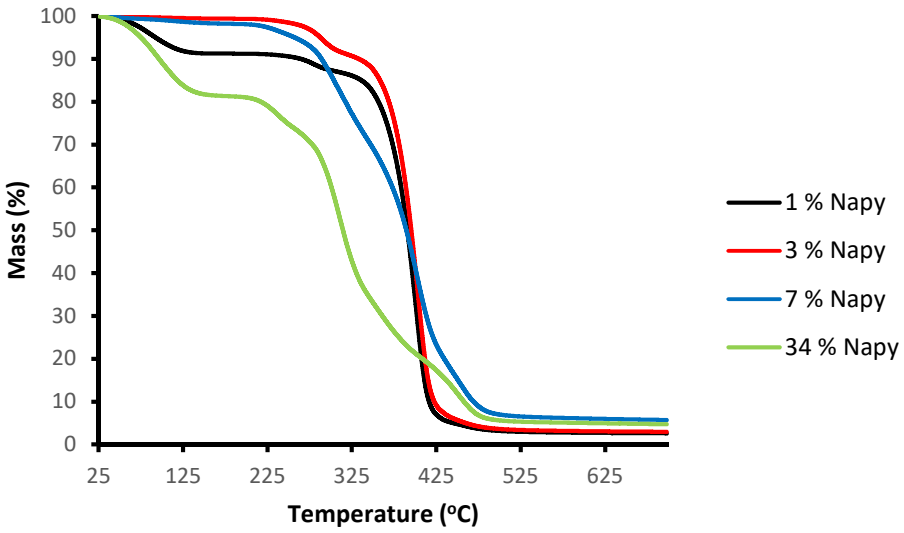

Figure 21. TGA for the different compositions of copolymer **15**

Conclusions

The aim of this research was to synthesize and characterize a supramolecular star core and a supramolecular brush polymer. In the first step of the synthesis of the supramolecular star core, triglycidyl ether **1** has reacted with sodium azide to form compound **2**. After extraction the product was obtained in high purity with a yield of 58 %. In the second step, the CuAAC click reaction was performed to attach the thymine-based sticker **3** to the star core **2**. The aim was to synthesize compound **4**, which contains a thymine end group on each of the three-arms. From ^{1}H NMR analysis a conversion of the click reaction of 53% could be determined. This means that most supramolecular star cores contained one or two thymine end groups on average. Since the conversion was low and the attempt to isolate the product by column chromatography failed, the supramolecular star core could not be used to form a supramolecular star network.

The supramolecular brush polymer was synthesized starting from the synthesis of the Napy-based sticker. In the first step of the synthesis of the sticker, 2,6-amino pyridine **6** has reacted with DL-malic acid **7** under acidic circumstances to give compound **8**, which was obtained quantitative and with high purity. In the next step compound **8** reacted with HDI **9** to give compound **10**. This product was also obtained quantitative. Although the remaining HDI **9** was evaporated by a vacuum distillation at 130 °C for several hours, the product still contained HDI **9**. But since an excess of 2-hydroxyethyl acrylate **11** was used in the next step, this was not problematic. ^{1}H NMR analysis confirms the formation of monomer **12** after 2-hydroxyethyl acrylate **11** was added to compound **10**. The Napy monomer was obtained pure in a 66% yield.

The Napy monomer was used to perform several polymerizations. Using DDMAT as CTA during Raft polymerization a polymer with $\overline{M_n}$ = 4,050 g/mol, calculated from ^{1}H NMR analysis, was synthesized. GPC could not be used to confirm the molecular weights and to determine the PDI values, since the polymer showed no solubility in THF or DMF and GPC measurements in DMSO were not possible. Also, MALDI ToF measurements did not succeed due to low solubility of the polymer. TGA and DSC confirmed that a high T_g polymer was obtained with $T_{d(max)}$ = 238.4 °C.

The Napy monomer **12** was also successfully used to produce a copolymer with different compositions of n-butyl acrylate. DSC measurements confirmed that increasing the number of Napy side groups in the copolymer, the T_g also increases, but the T_g values of the Napy copolymers were lower than the values of a similar copolymer containing UPy. TGA showed that the different Napy copolymers had $T_{d(max)}$ values around 400 °C.

For further research it is desirable to first confirm the formation of the Napy polymer by GPC in DMSO, also the molecular weights and PDI values can be determined in this way. After this, the Napy-based polymer and copolymers can be used to for the hydrogen bonding backbone in a supramolecular brush shaped network with linear side chains based on UPy (figure 6). This supramolecular network can be studied to introduce new properties to the field of supramolecular polymer chemistry.

Experimental

Nuclear magnetic resonance (NMR)

For the characterization of the synthesized compounds ^{1}H NMR analysis was performed with a Varian As 400 spectrometer. The samples were analysed in chloroform-d_1 and dimethylsulfoxide-d_6 was used when the compounds showed poor solubility in chloroform. The peak shifts were recorded in ppm (δ) and the samples were measured from -1 to 14 ppm. Most spectra show a shorter range, but this is because no peaks are visible outside this range. The FID-files were analysed with MestReNova (v11.0)

Gel permeation chromatography (GPC)

The GPC samples were prepared in THF (1 mg/ml) and were measured with a Viscotek. Polystyrene (PS) was used as internal standard (Mp=1-300kDa). Omisec (v5.0.2) was used to analyse the data (dn/dc = 0.064).

Differential scanning calorimetry (DSC)

A TA-instruments Q1000 differential scanning calorimeter was used for the calorimetric measurements. A temperature range of – 65 °C to 150 °C with a scanning rate of 40 °C min^{-1} was used for the measurements of the samples. The second heating ramp is displayed in the DSC graphs in the report, unless indicated otherwise.

Thermogravimetric analysis (TGA)

The thermal stability and the decomposition behaviour were determined with a TA-instruments D2500. A range from 25 °C to 750 °C was measured with a heating rate of 10 °C min^{-1}. The maximum rate of weight loss was assigned as the $T_{d(max)}$. The TGA curves were analysed with TRIOS software (v4.1) (TA Instruments).

Melt rheology

The rheological properties of the copolymers were measured with a TA Instruments AR 1000 melt rheometer. The samples were analysed using 8 mm diameter parallel plate geometry, with a gap setting of 500 µm. The measurements were performed with a 1 Hz frequency, 10 µN·m and temperature steps of 1 °C.

*Reaction 1.1: Synthesis of 3,3'-((2-((3-azido-2-hydroxypropoxy)methyl)-2-ethylpropane-1,3-diyl)bis(oxy))bis(1-azidopropan-2-ol) **2***

Ammonium chloride 1.79 g (33.5 mmol) and sodium azide 2.17 g (33.4 mmol) were added to a 100 mL three necked round bottom flask equipped with stirring egg. Next 30 mL methanol and 2.00 g trimethylolpropane triglycidyl ether **1** (6.61 mmol) were added to the reaction flask. The reaction mixture was stirred and heated to reflux for 19 h. After the reaction was finished, methanol was removed under reduced pressure and the crude product was obtained. 20 mL chloroform was used to dissolve the crude product. The solution was transferred to a separatory funnel and was washed with water (2 x 20 mL) and brine (1 x 10 mL). The organic layer was dried over magnesium sulphate and the chloroform was removed under reduced pressure to give a yellow oil (yield = 58 %). ^{1}H NMR (400 MHz, $CDCl_3$) ppm 3.94 (m, $3H_5$), 3.48 (m, $18H_{3,4,7}$), 2.77 (s, $3H_6$), 1.39 (m, $2H_2$), 0.85 (t, $3H_1$).

*Reaction 1.2: Click reaction between 3,3'-((2-((3-azido-2-hydroxypropoxy)methyl)-2-ethylpropane-1,3-diyl)bis(oxy))bis(1-azidopropan-2-ol) **2** and 5-methyl-1-(prop-2-yn-1-yl)pyrimidine-2,4(1H,3H)-dione **3***

For the click reaction 0.513 g 5-methyl-1-(prop-2-yn-1-yl)pyrimidine-2,4(1H,3H)-dione **3** (3.13 mmol), 0.102 g sodium ascorbate (0.515 mmol) and 0.0517 g $Cu(SO_4).5H_2O$ (0.207 mmol) were added to a 25 mL three necked round bottom flask equipped with stirring egg and Schlenk line. After putting the reaction flask under nitrogen atmosphere, 5.7 mL dry DMF and 0.300 g 3,3'-((2-((3-azido-2-hydroxypropoxy)methyl)-2-ethylpropane-1,3-diyl)bis (oxy))bis(1-azidopropan-2-ol) **2** (0.695 mmol) where added to the reaction flask. After 24 h the reaction was stopped by pouring the reaction mixture into a 150 mL HCL solution (0.1 M). The product was extracted from the aqueous layer by DCM (3 x 50 mL). From ^{1}H NMR it can be concluded that the product was obtained with a 53 % conversion.

*Reaction 2.1: Synthesis of 7-amino-1,8-naphthyridin-2(1H)-one **8***

45 mL concentrated sulfuric acid (97 %) was added dropwise to a ground mixture of 10.0 g 2,6-aminopyridine **6** (102 mmol) and 12.3 g DL-malic acid **7** (91.7 mmol) while keeping the flask in an ice bath. After all sulfuric acid was added, the mixture was heated to 110 °C. After 3.5h of heating, the mixture was allowed to cool down to 0 °C. Around 160 mL ammonium chloride (27 %) was added dropwise to the mixture until a pH of 9-10. The precipitate was filtered off and was washed with water (3 x 50 mL). The product was allowed to dry in a vacuum oven (40 °C). The product was obtained quantitative. ^{1}H NMR (400 MHz, DMSO) ppm 11.73 (s, $1H_1$), 7.61 (m,$2H_{2,5}$), 6.89 (s, $2H_6$), 6.33 (d, $1H_3$), 6.10 (d, $1H_4$).

*Reaction 2.2: Synthesis of 1-(6-isocyanatohexyl)-3-(7-oxo-7,8-dihydro-1,8-naphthyridin-2-yl)urea **10***

All 7-amino-1,8-naphthyridin-2(1H)-one **8** (91.700 mmol) from the previous reaction was added to a 500 mL three-necked round bottom flask. The solids were allowed to dry for one hour under vacuum. The flask was put under nitrogen atmosphere by vacuum/nitrogen cycles (3x). 200 mL HDI **9** (1.25 mol) was added to the reaction flask. The reaction mixture was heated to 110 °C while stirring. After 19h the reaction was stopped by letting the reaction mixture cool down to room temperature. The reaction mixture was precipitated in 500 mL hexane. The precipitate was filtered off, and the product was obtained as a light brown solid, which still contained HDI **9**. The product was obtained quantitative by distilling the HDI **9** off under reduced pressure at 130 °C for 6h. ^{1}H NMR (400 MHz, DMSO) ppm 12.15 (s, 1H$_1$), 9.63 (t, 1H$_6$), 8.98 (m, 1H$_7$), 7.88 (d, 1H$_4$), 7.75 (d, 1H$_3$), 6.83 (d, 1H$_5$), 6.31 (d, 1H$_2$), 3.18 (m, 4H$_{8,13}$), 1.33 (m, 8H$_{9\text{-}12}$).

*Reaction 2.3: Synthesis of 2-(((6-(3-(7-oxo-7,8-dihydro-1,8-naphthyridin-2-yl)ureido)hexyl)carbamoyl)oxy)ethyl acrylate **12***

1.420 g 1-(6-isocyanatohexyl)-3-(7-oxo-7,8-dihydro-1,8-naphthyridin-2-yl)urea **10** (4.310 mmol) was added under nitrogen atmosphere to 250 mL three-necked round bottom flask. The solids where dried by vacuum/nitrogen cycles (3x). 75 mL dry chloroform was added to the flask and the mixture was stirred obtaining a yellow suspension. 2.625 g 2-hydroxyethylacrylate **11** (22.606 mmol) and 15 droplets dibutyltin dilaurate were added to the stirred suspension. The mixture was heated to reflux for 6h. The reaction was stopped by cooling the reaction mixture down to room temperature. The product was precipitate in 400 mL hexane. The precipitate was filtered off and was dissolved in 10 mL DMSO. The solution was precipitated in 200 mL water. The precipitate was filtered off and was allowed to dry overnight in a vacuum oven (40 °C). The product was obtained as dark brown solid aggregates (yield = 66 %). ^{1}H NMR (400 MHz, $CDCl_3$) ppm 8.03 (s, 1H$_5$), 7.84 (d, 1H$_4$), 7.73 (d, 1H$_3$), 6.54 (d, 1H$_2$), 6.41 (d, 1H$_{19}$), 6.15 (m, 1H$_{17}$), 5.87 (d, 2H$_{18}$), 4.85 (s, 1H$_{14}$), 4.33 (m, 4H$_{15,16}$), 3.32 (q, 2H$_{13}$), 3.18 (q, 2H$_8$), 1.41 (m, 8H$_{9\text{-}12}$).

Table 2. Conditions for reaction 2.3

Reaction	Compound 10		Compound 11		DBDTL	Chloroform	Temperature	Reaction time	Yield
	g	mmol	g	mmol	drops	mL	°C	hours	%
2.3.1	0.185	0.562	0.322	2.773	2	10	65	6	42
2.3.2	0.550	1.670	0.966	8.319	6	30	65	6	38
2.3.3	1.420	4.310	2.625	22.606	15	75	65	6	66
2.3.4	6.030	18.30	10.309	88.779	60	300	65	6	68

*Reaction 3.1: Raft polymerization of 2-(((6-(3-(7-oxo-7,8-dihydro-1,8-naphthyridin-2-yl)ureido)hexyl)carbamoyl)oxy)ethyl acrylate **12***

0.250 g of 2-(((6-(3-(7-oxo-7,8-dihydro-1,8-naphthyridin-2-yl)ureido)hexyl)carbamoyl)oxy) ethyl acrylate **12** (0.561 mmol) was added under nitrogen to a pre-dried Schlenk tube equipped with magnetic stirrer. 25 mL dry DMSO was added to the Schlenk tube. 0.011 g DDMAT (0.030 mmol) and 0.492 mg AIBN (0.003 mmol) were added from a stock solution in DMSO. After applying 15 minutes of vacuum, the reaction mixture was stirred in a 65 °C oil batch for 6h. The reaction was quenched by putting the Schlenk tube in liquid nitrogen. The reaction mixture was precipitated in 300 mL methanol. The polymer was obtained as a yellow-brown solid. ^{1}H NMR (400 MHz, $CDCl_3$) ppm 12.16 (s, H_1), 9.61 (d, $1H_6$), 8.96 (s, $1H_7$), 7.88 (d, $1H_4$), 7.75 (d, $1H_3$), 6.81 (d, $1H_5$), 6.33 (d, $1H_2$), 4.14 (m, $4H_{15,16}$), 3.05 (m, $4H_{8\text{-}13}$), 1.27 (m, $8H_{9\text{-}12}$), 0.81 (s, $3H_{17}$).

Table 3. Conditions for reaction 3.1

Reaction	Compound 12		CTA		DMSO	Temperature	Reaction time
	g	mmol		mmol	mL	°C	hours
3.1.1	0.234	0.525	DBTTC	0.007	25	65	21
3.1.2	0.250	0.561	DBTTC	0.008	25	65	6
3.1.3	0.250	0.561	DDMAT	0.030	25	65	6
3.1.4	0.500	1.122	DDMAT	0.038	50	65	6

*Reaction 3.2: Copolymerization of n-butyl acrylate and 2-(((6-(3-(7-oxo-7,8-dihydro-1,8-naphthyridin-2-yl)ureido)hexyl)carbamoyl)oxy)ethyl acrylate **12***

0.447 g 2-(((6-(3-(7-oxo-7,8-dihydro-1,8-naphthyridin-2-yl)ureido)hexyl)carbamoyl)oxy)ethyl acrylate **12** (1.003 mmol) and 1.154 g n-butyl acrylate **14** (9.003 mmol) were added to a reaction flask equipped with stirring egg. 0.010 g DBTTC and 0.547 mg AIBN were added to the monomer mixture. 5 mL dry DMSO was added, and all the components were mixed. 15 minutes of vacuum were applied to get rid of all oxygen. The reaction mixture was heated to 65 °C for 6 hours. The reaction mixture was precipitated a 100 mL methanol : water (80 : 20) mixture. After centrifugation the precipitate was obtained as a yellow solid. ^{1}H NMR (400 MHz, DMSO) ppm 12.16 (s, $1H_1$), 9.61 (d, $1H_6$), 8.96 (s, $1H_7$), 7.88 (d, $1H_4$), 7.77 (d, $1H_3$), 6.83 ($1H_5$), 6.31 (d, $1H_2$), 1.33 (m, $7H_{17,18,19}$).

Table 4. Conditions for reaction 3.2

Reaction	Compound 12		n-Butyl acrylate		DMSO	Temperature	Reaction time
	g	mmol	g	mmol	mL	°C	hours
3.2.1	0.447	1.003	1.154	9.003	5.0	65	6
3.2.2	1.330	2.986	0.897	7.000	10.0	65	6
3.2.3	0.000	0.000	1.280	9.986	0.0	65	6
3.2.4	0.134	0.301	1.243	9.697	1.5	65	6
3.2.5	0.045	0.101	1.269	9.900	1.0	65	6

References

[1] S. I. Stupp and L. C. Palmer, “Supramolecular chemistry and self-assembly in organic materials design,” *Chem. Mater.*, vol. 26, no. 1, pp. 507–518, 2014.

[2] A. I. Berg and K. U. Loos, “Supramolecular polymers for biomedical applications.”

[3] D. W. R. Balkenende, C. A. Monnier, G. L. Fiore, and C. Weder, “Optically responsive supramolecular polymer glasses,” *Nat. Commun.*, vol. 7, pp. 1–9, 2016.

[4] S. Sivakova, D. A. Bohnsack, M. E. Mackay, P. Suwanmala, and S. J. Rowan, “Utilization of a combination of weak hydrogen-bonding interactions and phase segregation to yield highly thermosensitive supramolecular polymers,” *J. Am. Chem. Soc.*, vol. 127, no. 51, pp. 18202–18211, 2005.

[5] T. Aida, E. W. Meijer, and S. I. Stupp, “Functional supramolecular polymers,” *Science (80-.).*, vol. 335, no. 6070, pp. 813–817, 2012.

[6] D. Zhang *et al.*, “Hierarchical Self-Assembly of a Dandelion-Like Supramolecular Polymer into Nanotubes for use as Highly Efficient Aqueous Light-Harvesting Systems,” *Adv. Funct. Mater.*, vol. 26, no. 42, pp. 7652–7661, 2016.

[7] T. Park and S. C. Zimmerman, “Formation of a miscible supramolecular polymer blend through self-assembly mediated by a quadruply hydrogen-bonded heterocomplex,” *J. Am. Chem. Soc.*, vol. 128, no. 35, pp. 11582–11590, 2006.

[8] A. Shaygan Nia, S. Rana, D. Döhler, W. Osim, and W. H. Binder, “Nanocomposites via a direct graphene-promoted ‘click’-reaction,” *Polym. (United Kingdom)*, vol. 79, pp. 21–28, 2015.

[9] L. Balacca, E. Van Ruymbeke, S. Coppola, S. Righi, and D. Vlassopoulos, “Decoding the viscoelastic response of polydisperse star/linear polymer blends,” *AIP Conf. Proc.*, vol. 1027, no. May 2014, pp. 418–420, 2008.

[10] H. C. Kolb and K. B. Sharpless, “The growing impact of click chemistry on drug discovery,” *Drug Discov. Today*, vol. 8, no. 24, pp. 1128–1137, 2003.

[11] B. T. Worrell, J. A. Malik, and V. V Fokin, “Direct Evidence of a Dinuclear Copper Intermediate in Cu(I)-Catalyzed Azide-Alkyne Cycloadditions,” *Science (80-.).*, vol. 340, no. 6131, p. 457 LP-460, Apr. 2013.

[12] G. Moad, Y. K. Chong, A. Postma, E. Rizzardo, and S. H. Thang, “Advances in RAFT polymerization: The synthesis of polymers with defined end-groups,” *Polymer (Guildf).*, vol. 46, no. 19 SPEC. ISS., pp. 8458–8468, 2005.

[13] L. Brunsveld, B. J. B. Folmer, E. W. Meijer, and R. P. Sijbesma, “Supramolecular Polymers,” *Chem. Rev.*, vol. 101, no. 12, pp. 4071–4098, Dec. 2001.

[14] L. J., V. J. A., W. M. H., and A. M., “Shape-Memory Effects in Polymer Networks Containing Reversibly Associating Side-Groups,” *Adv. Mater.*, vol. 19, no. 19, pp. 2851–2855, Sep. 2007.

[15] L. Leibler, M. Rubinstein, and R. H. Colby, “Dynamics of reversible networks,” *Macromolecules*, vol. 24, no. 16, pp. 4701–4707, Aug. 1991.

[16] S. Sivakova and S. J. Rowan, “Nucleobases as supramolecular motifs,” *Chem. Soc. Rev.*, vol. 34, no. 1, pp. 9–21, 2005.

[17] C. G. Burd, “Supramolecular Block and Random Copolymers in Multifunctional Assemblies,” *Dissertation*, no. August, 2008.

[18] P. Y. W. Dankers *et al.*, “Hierarchical formation of supramolecular transient networks in water: A modular injectable delivery system,” *Adv. Mater.*, vol. 24, no. 20, pp. 2703–2709, 2012.

[19] C. L. Lewis, K. Stewart, and M. Anthamatten, “The influence of hydrogen bonding side-groups on viscoelastic behavior of linear and network polymers,” *Macromolecules*, vol. 47, no. 2, pp. 729–740, 2014.

[20] C. Chemistry, “Click Chemistry background information Principle of Click Chemistry 1. Activation of molecule A and B Compatible CLICK-functional groups are introduced via CLICK Reagents 2. CLICK-coupling of molecule A and B The CLICK-activated molecules A and B form a s,” 2017.

Supplementary information

1 *[1]H NMR spectrum of reaction 3.1.2*

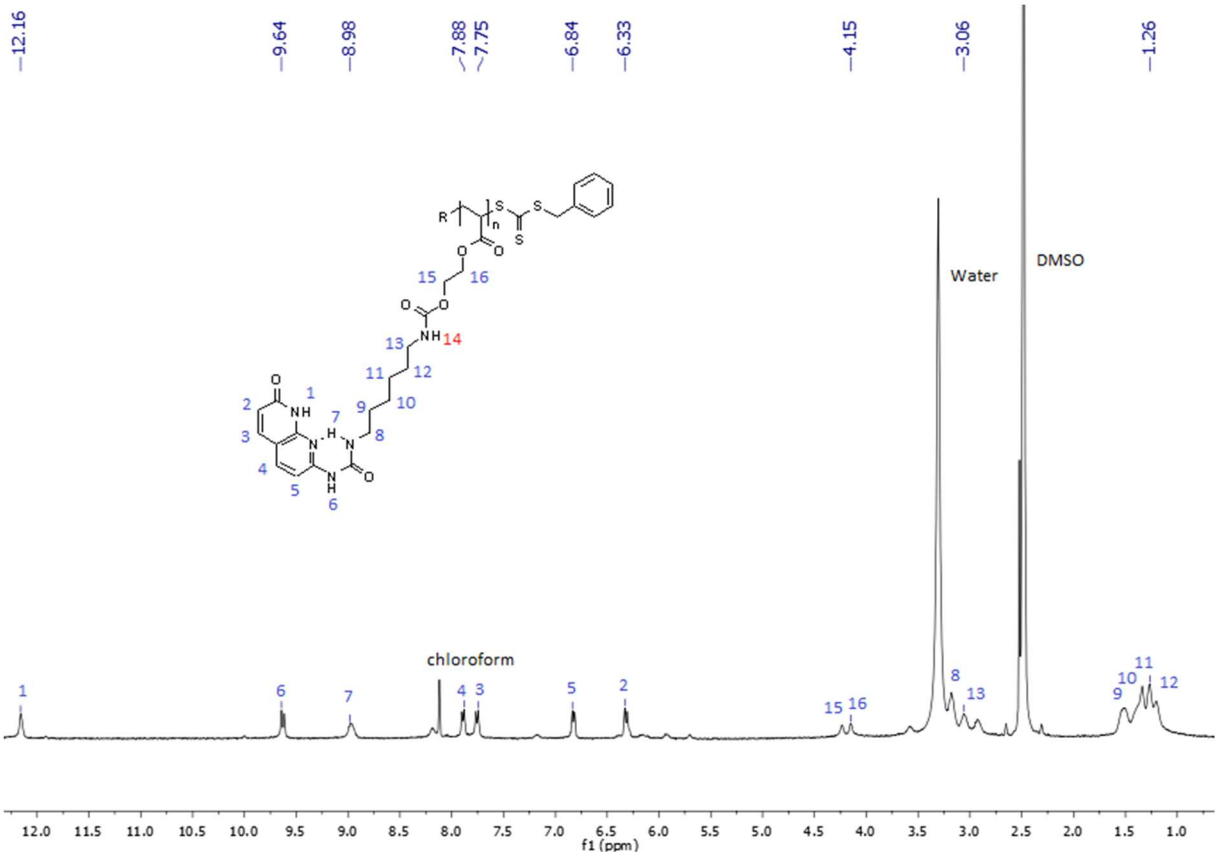

Figure S1. [1]H NMR spectrum of the polymerization of compound **12** with DBTTC used as CTA with aimed $\overline{M_n} = 20{,}000$

2 ^{1}H NMR spectrum of reaction 3.1.4

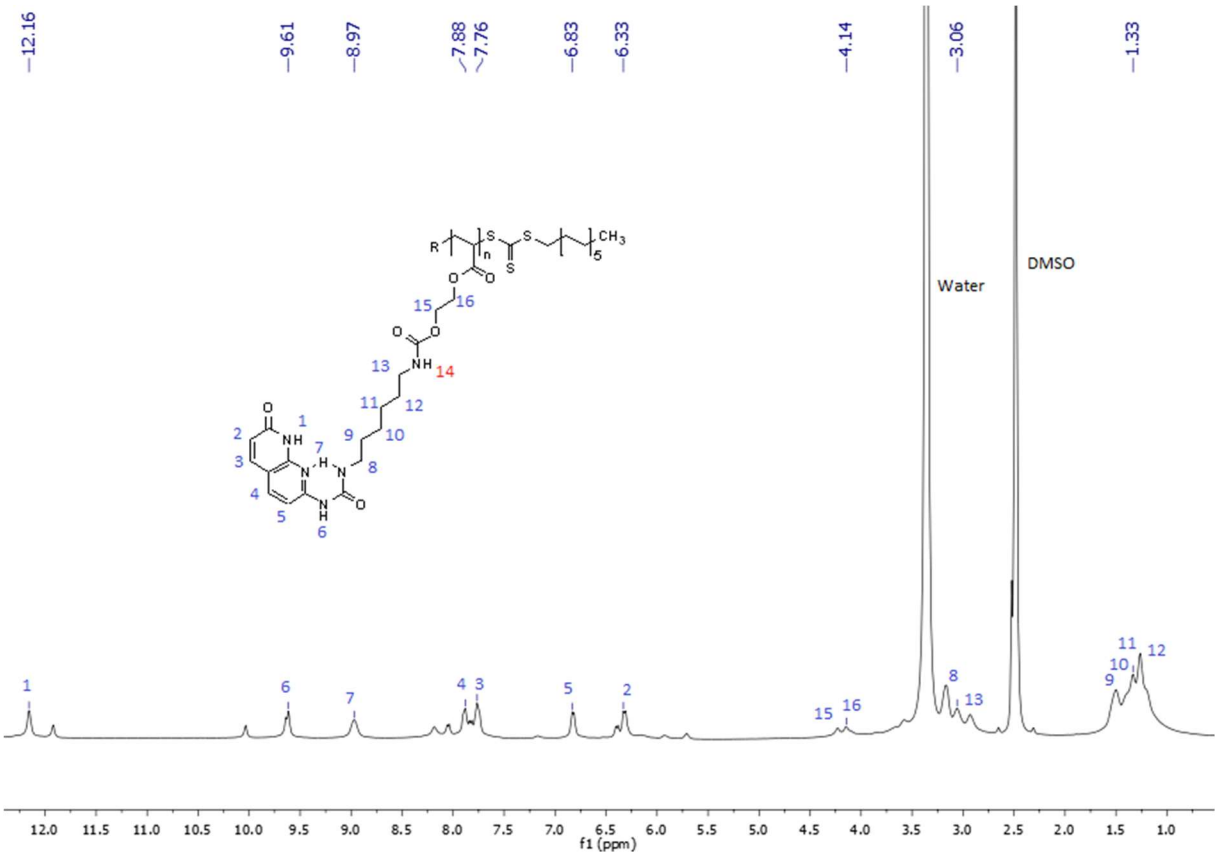

Figure S2. ^{1}H NMR spectrum of the polymerization of compound **12** with DDMAT used as CTA with aimed $\overline{M_n} = 80{,}000$

3 ^{1}H NMR spectrum of reaction 3.2.2

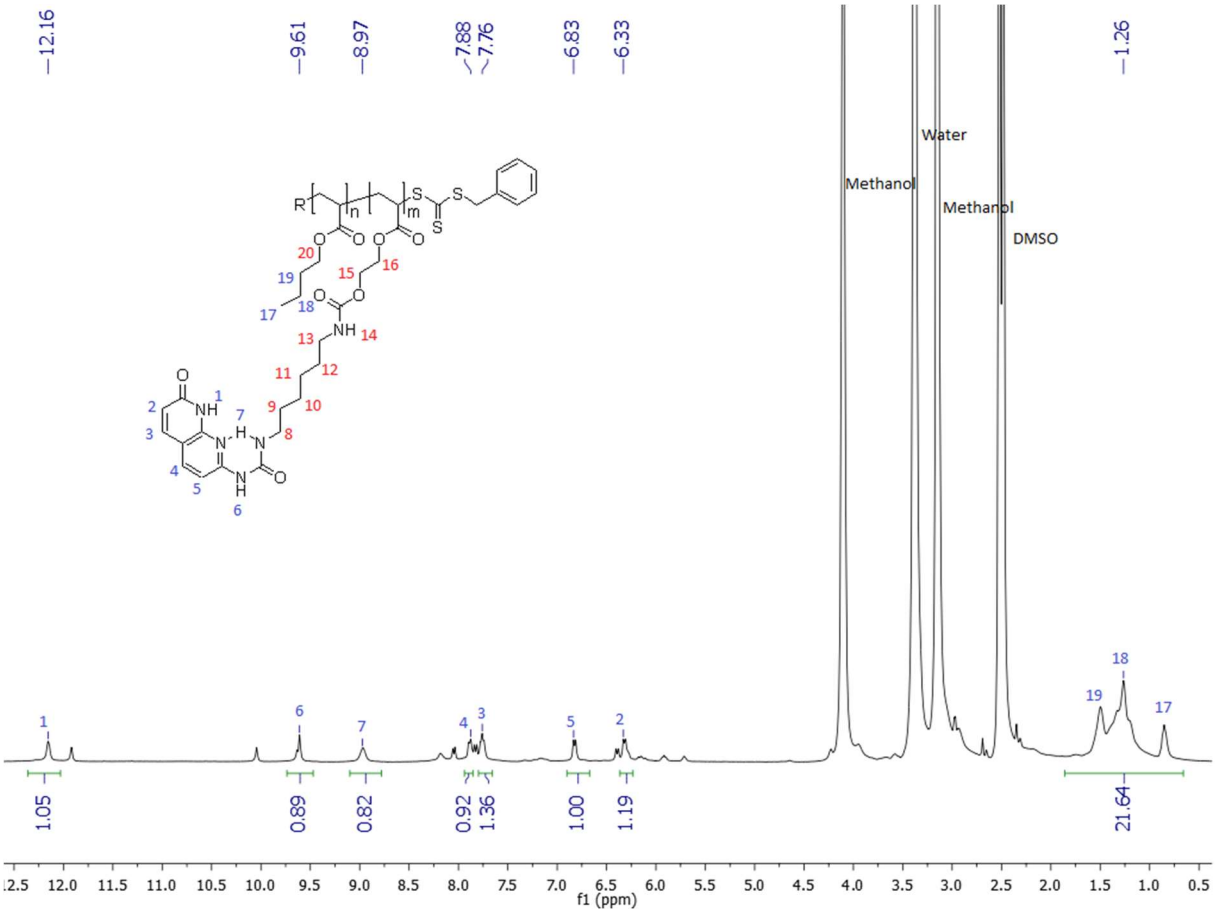

Figure S3. ^{1}H NMR spectrum of the copolymerization of compound **12** (30 %) and compound **14** (70 %) with DBTTC used as CTA.

4 ^{1}H NMR spectrum of reaction 3.2.4

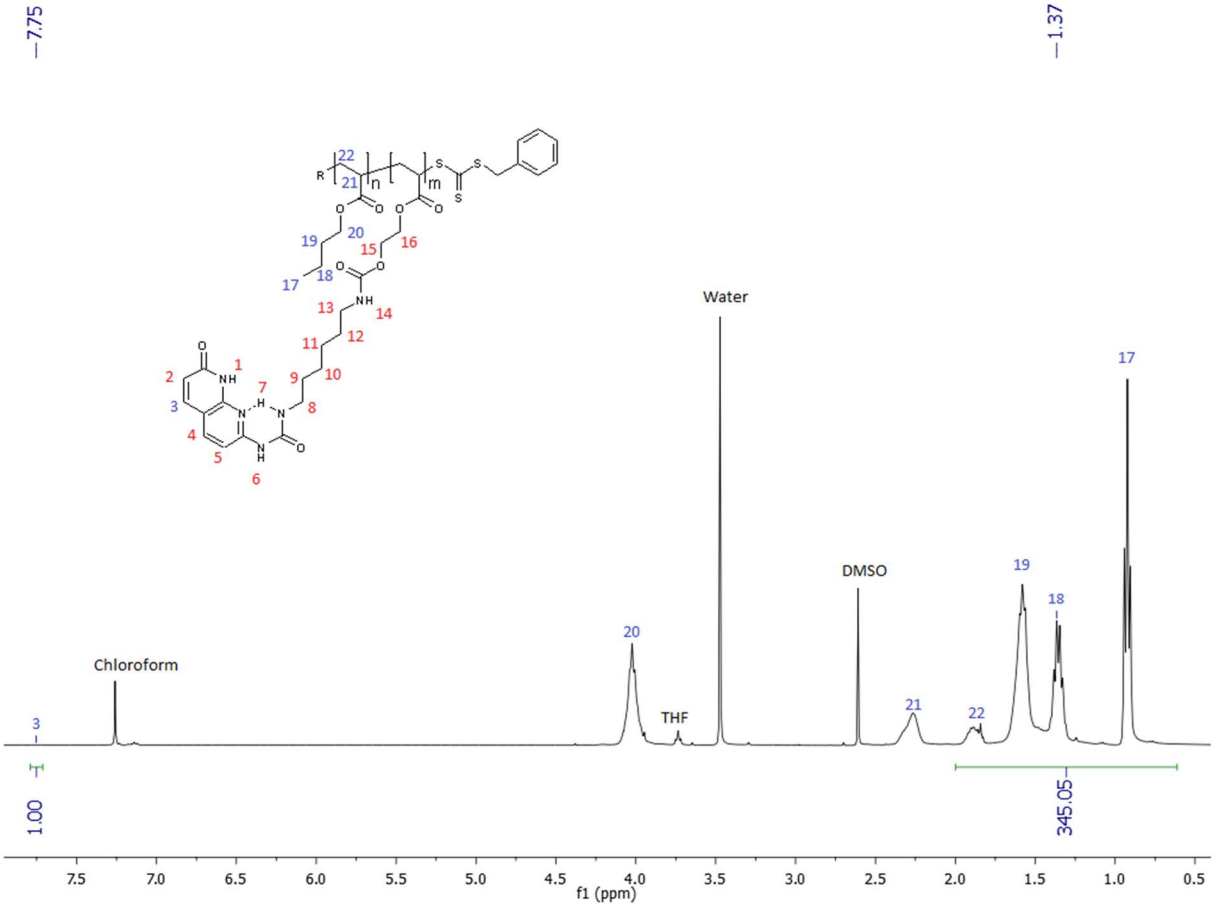

Figure S4. ^{1}H NMR spectrum of the copolymerization of compound **12** (3 %) and compound **14** (97%) with DBTTC used as CTA.

5 [1]H NMR spectrum of reaction 3.2.4

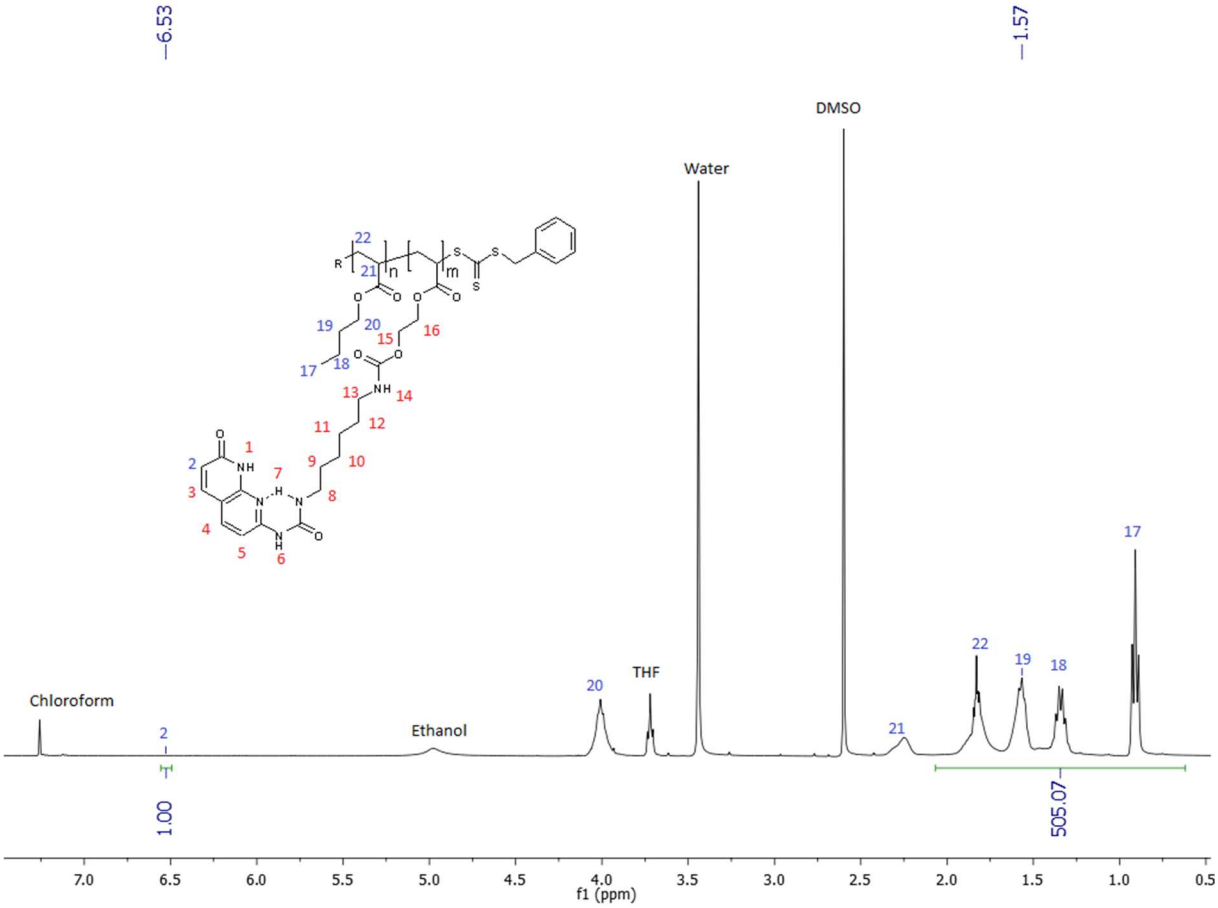

Figure S5. [1]H NMR spectrum of the copolymerization of compound **12** (1 %) and compound **14** (99 %) with DBTTC used as CTA.

*6 TGA of polymer **13** with $\overline{M_n}$ = 4,050 g/mol*

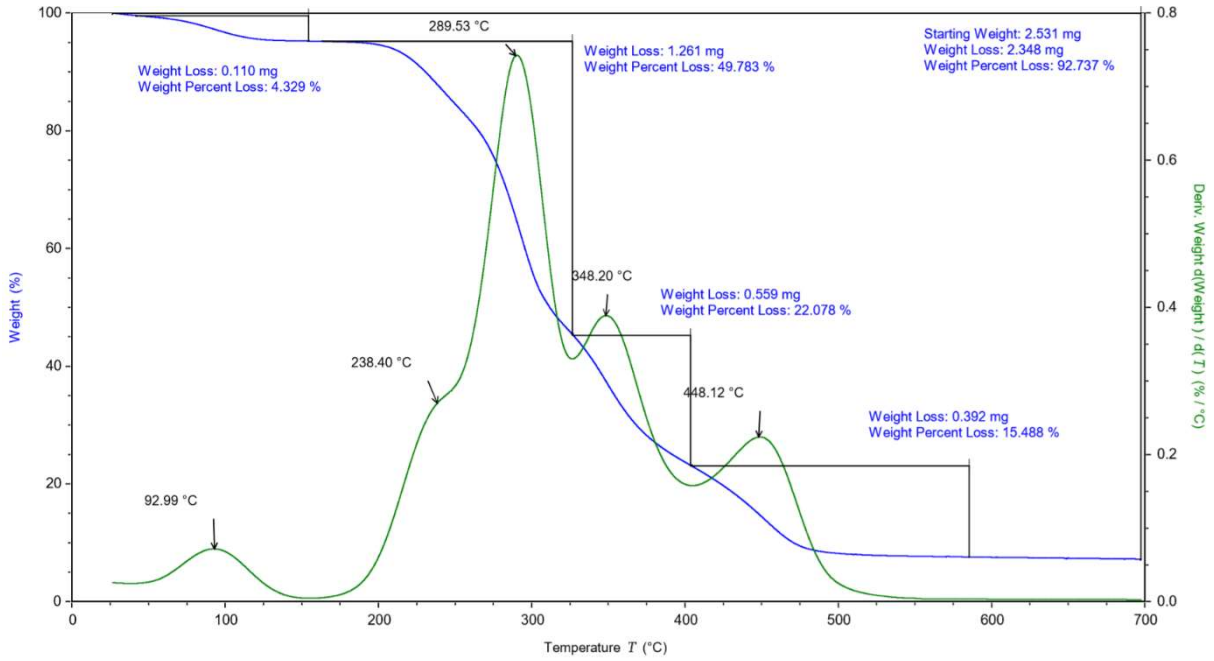

Figure S6. TGA of polymer **13** with $\overline{M_n}$ = 4,050 g/mol

*7 TGA of polymer **13** with aimed $\overline{M_n}$ = 20,000 g/mol*

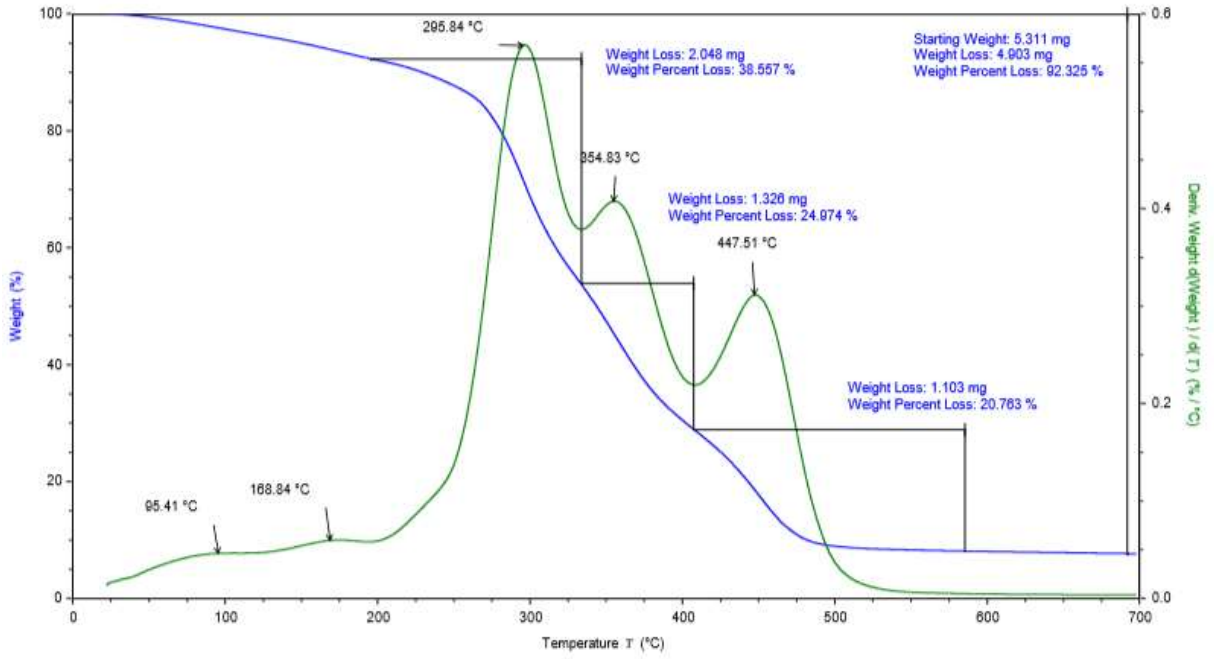

Figure S7. TGA of polymer **13** with $\overline{M_n}$ = 20,000 g/mol

*8 TGA of copolymer **15** with 1 % Napy*

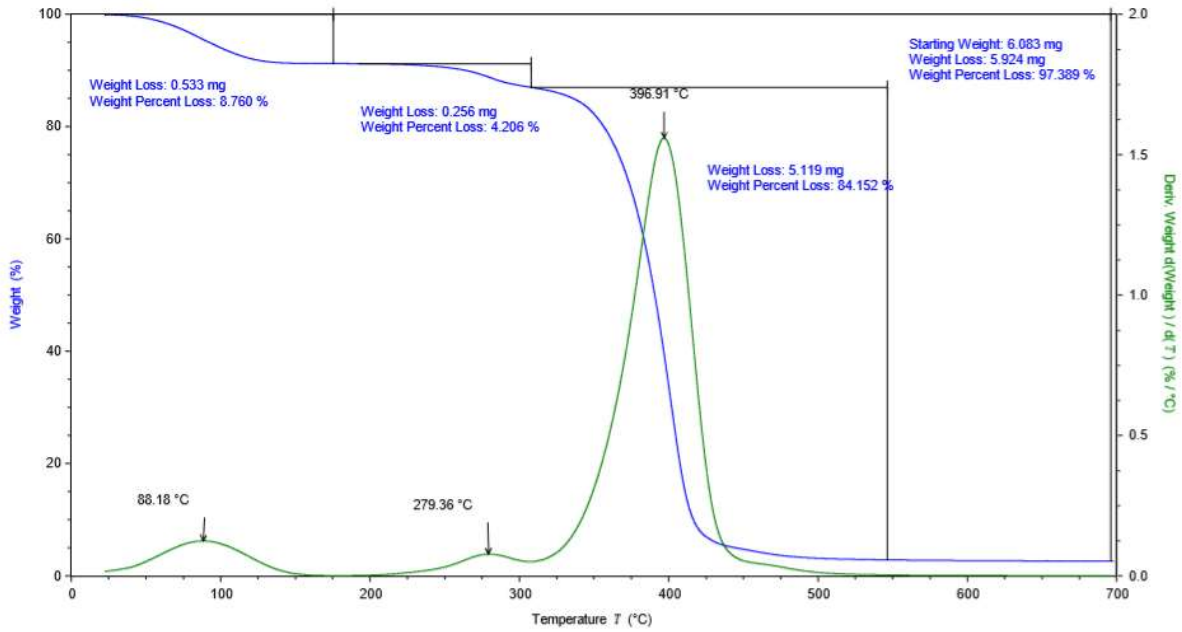

Figure S8. TGA of copolymer **15** with 1 % Napy

*9 TGA of copolymer **15** with 3 % Napy*

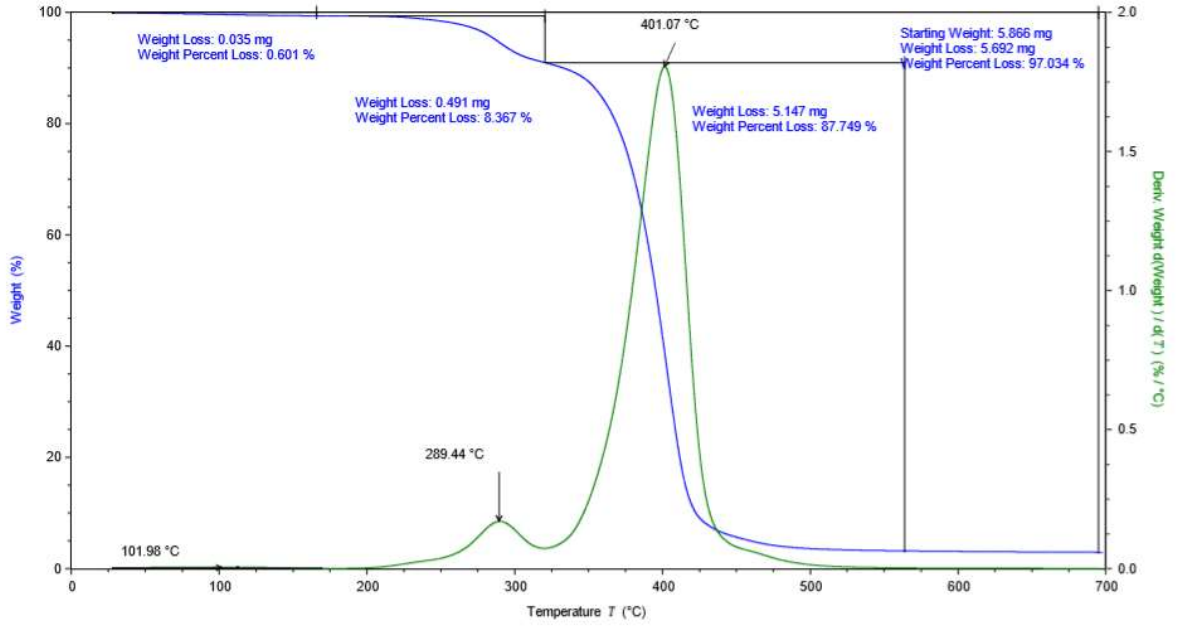

Figure S9. TGA of copolymer **15** with 3 % Napy

*10 TGA of copolymer **15** with 7 % Napy*

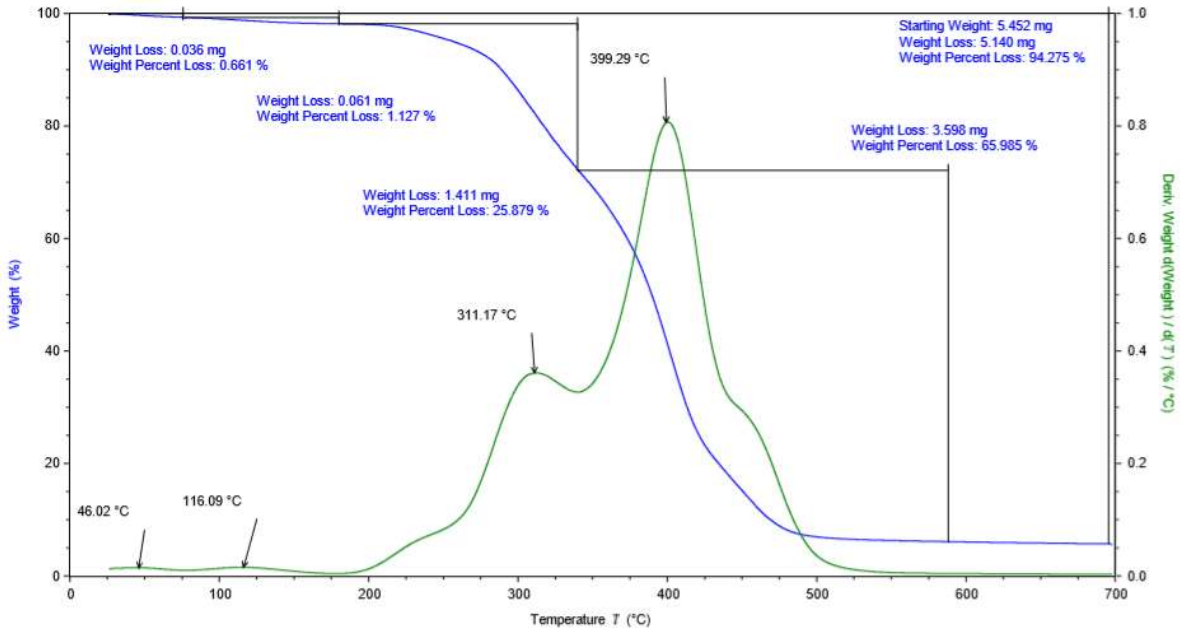

Figure S10. TGA of copolymer **15** with 7 % Napy

*11 TGA of copolymer **15** with 34 % Napy*

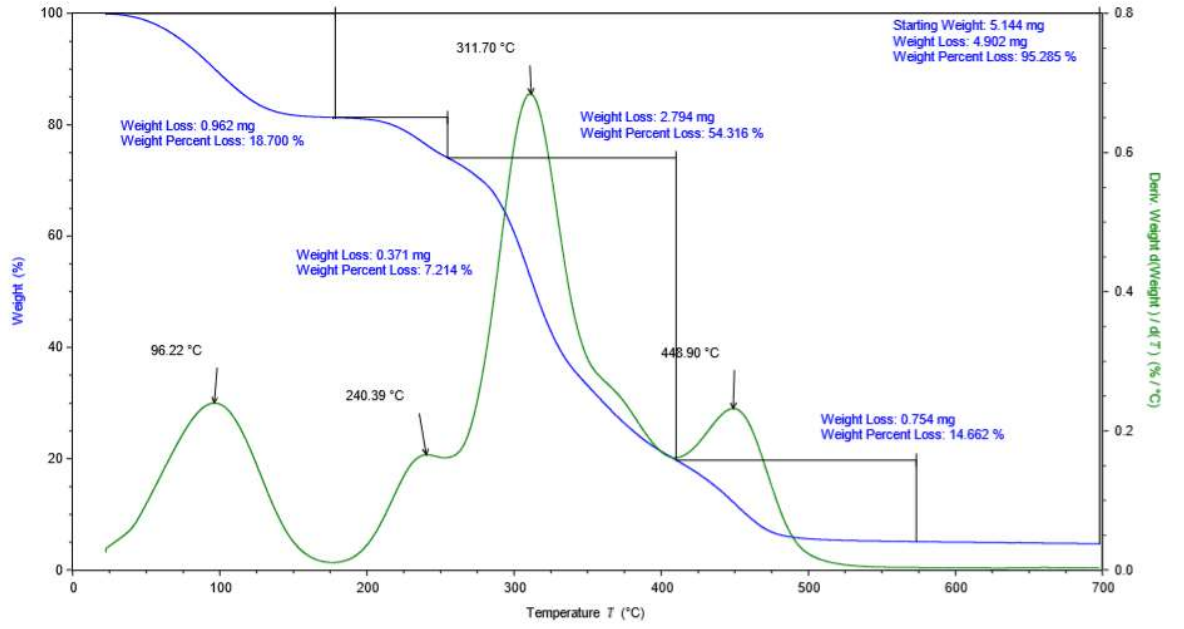

Figure S11. TGA of copolymer **15** with 34 % Napy

*12 Rheology of copolymer **15** from 10 % monomer **12** and 90 % monomer **14***

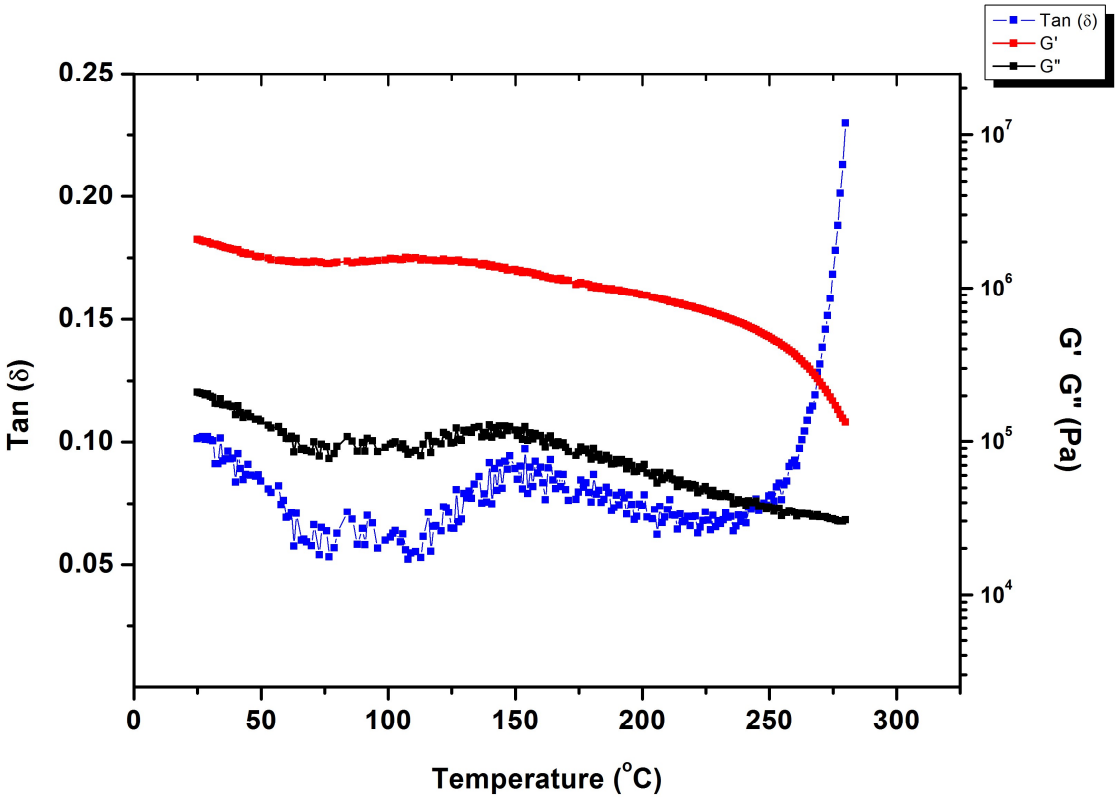

Figure S8. Rheology of copolymer **15** from 10 % monomer **12** and 90 % monomer **14**

13 Thermal properties of copolymers containing Napy and UPy

HB	X_{HB}	T_g
	Mole %	°C
UPy	0	-49.0
UPy	1	-46.5
UPy	2	-43.6
UPy	5	-38.7
Napy	0	-49.2
Napy	1	-48.9
Napy	3	-46.9
Napy	7	-42.8
Napy	34	27.5

Table S1. Thermal properties of copolymers of n-butyl acrylate and different compositions of the hydrogen bonding groups (X_{HB}) UPy and Napy